

---

# **Rock Engineering:** *Underground Openings*

Course No: G05-004

Credit: 5 PDH

---

Yun Zhou, PhD, PE

---



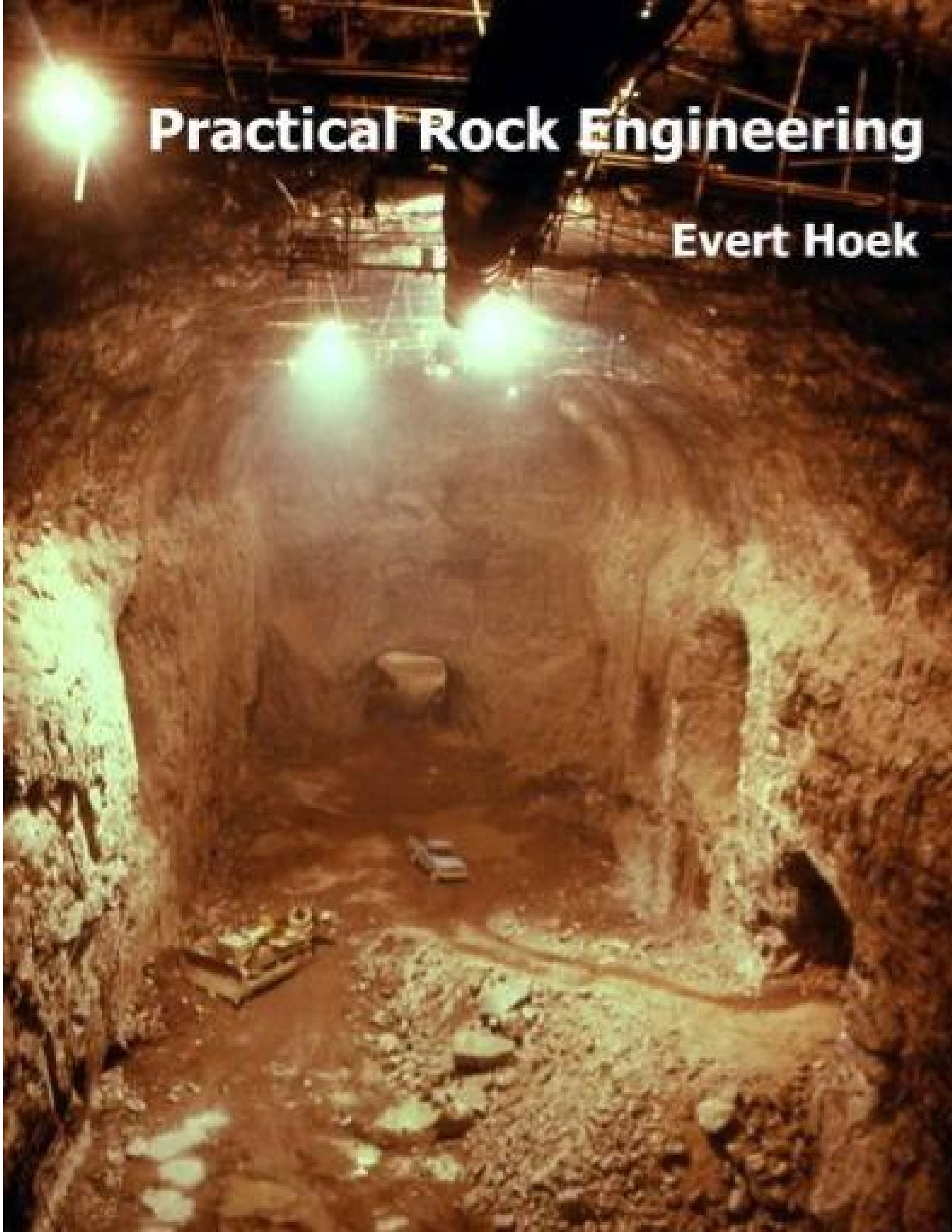
Continuing Education and Development, Inc.  
22 Stonewall Court  
Woodcliff Lake, NJ 07677

P: (877) 322-5800  
[info@cedengineering.com](mailto:info@cedengineering.com)

---

# Practical Rock Engineering

Evert Hoek



# Preface

These notes were originally prepared during the period 1987 to 1993 for undergraduate and graduate courses in rock engineering at the University of Toronto. While some revisions were made in 2000 these were difficult because the notes had been formatted as a book with sequential chapter and page numbering. Any changes required reformatting the entire set of notes and this made it impractical to carry out regular updates.

In 2006 it was decided that a major revision was required in order to incorporate significant developments in rock engineering during the 20 years since the notes were originally written. The existing document was broken into a series of completely self-contained chapters, each with its own page numbering and references. This means that individual chapters can be updated at any time and that new chapters can be inserted as required.

The notes are intended to provide an insight into practical rock engineering to students, geotechnical engineers and engineering geologists. Case histories are used, wherever possible, to illustrate the methods currently used by practicing engineers. No attempt has been made to include recent research findings which have not yet found their way into everyday practical application. These research findings are adequately covered in conference proceedings, journals and on the Internet.

It is emphasised that these are notes are not a formal text. They have not been and will not be published in their present form and the contents will be revised from time to time to meet the needs of particular audiences.

Readers are encouraged to send their comments, corrections, criticisms and suggestions to me at the address given below. These contributions will help me to improve the notes for the future.



Dr Evert Hoek  
Evert Hoek Consulting Engineer Inc.  
3034 Edgemont Boulevard  
P.O. Box 75516  
North Vancouver, B.C.  
Canada V7R 4X1  
Email: [ehoek@mailas.com](mailto:ehoek@mailas.com)

# In situ and induced stresses

## Introduction

Rock at depth is subjected to stresses resulting from the weight of the overlying strata and from locked in stresses of tectonic origin. When an opening is excavated in this rock, the stress field is locally disrupted and a new set of stresses are induced in the rock surrounding the opening. Knowledge of the magnitudes and directions of these in situ and induced stresses is an essential component of underground excavation design since, in many cases, the strength of the rock is exceeded and the resulting instability can have serious consequences on the behaviour of the excavations.

This chapter deals with the question of in situ stresses and also with the stress changes that are induced when tunnels or caverns are excavated in stressed rock. Problems, associated with failure of the rock around underground openings and with the design of support for these openings, will be dealt with in later chapters.

The presentation, which follows, is intended to cover only those topics which are essential for the reader to know about when dealing with the analysis of stress induced instability and the design of support to stabilise the rock under these conditions.

## In situ stresses

Consider an element of rock at a depth of 1,000 m below the surface. The weight of the vertical column of rock resting on this element is the product of the depth and the unit weight of the overlying rock mass (typically about 2.7 tonnes/m<sup>3</sup> or 0.027 MN/m<sup>3</sup>). Hence the vertical stress on the element is 2,700 tonnes/m<sup>2</sup> or 27 MPa. This stress is estimated from the simple relationship:

$$\sigma_v = \gamma z \quad (1)$$

where  $\sigma_v$  is the vertical stress  
 $\gamma$  is the unit weight of the overlying rock and  
 $z$  is the depth below surface.

Measurements of vertical stress at various mining and civil engineering sites around the world confirm that this relationship is valid although, as illustrated in Figure 1, there is a significant amount of scatter in the measurements.

*In situ and induced stresses*

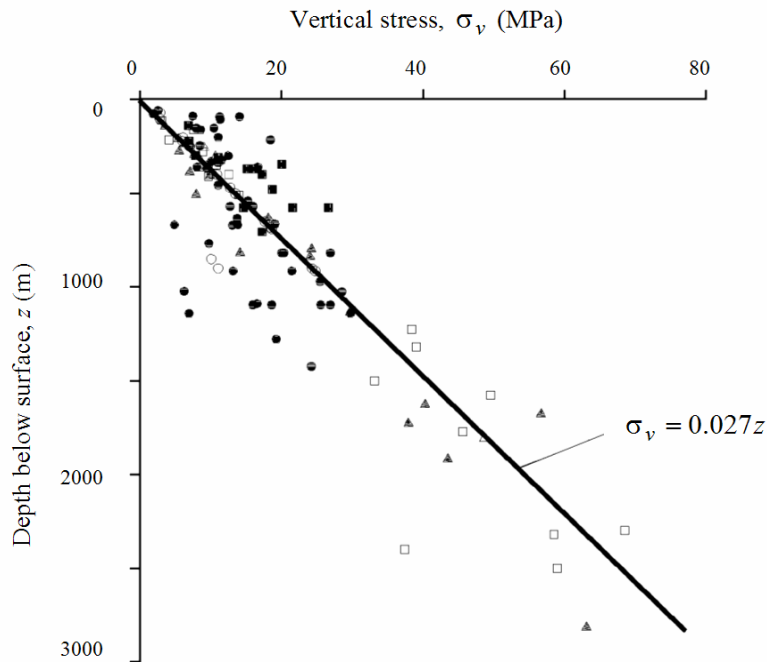


Figure 1: Vertical stress measurements from mining and civil engineering projects around the world. (After Brown and Hoek 1978).

The horizontal stresses acting on an element of rock at a depth  $z$  below the surface are much more difficult to estimate than the vertical stresses. Normally, the ratio of the average horizontal stress to the vertical stress is denoted by the letter  $k$  such that:

$$\sigma_h = k\sigma_v = k \gamma z \quad (2)$$

Terzaghi and Richart (1952) suggested that, for a gravitationally loaded rock mass in which no lateral strain was permitted during formation of the overlying strata, the value of  $k$  is independent of depth and is given by  $k = \nu/(1-\nu)$ , where  $\nu$  is the Poisson's ratio of the rock mass. This relationship was widely used in the early days of rock mechanics but, as discussed below, it proved to be inaccurate and is seldom used today.

Measurements of horizontal stresses at civil and mining sites around the world show that the ratio  $k$  tends to be high at shallow depth and that it decreases at depth (Brown and Hoek, 1978, Herget, 1988). In order to understand the reason for these horizontal stress variations it is necessary to consider the problem on a much larger scale than that of a single site.

*In situ and induced stresses*

Sheorey (1994) developed an elasto-static thermal stress model of the earth. This model considers curvature of the crust and variation of elastic constants, density and thermal expansion coefficients through the crust and mantle. A detailed discussion on Sheorey's model is beyond the scope of this chapter, but he did provide a simplified equation which can be used for estimating the horizontal to vertical stress ratio  $k$ . This equation is:

$$k = 0.25 + 7E_h \left( 0.001 + \frac{1}{z} \right) \quad (3)$$

where  $z$  (m) is the depth below surface and  $E_h$  (GPa) is the average deformation modulus of the upper part of the earth's crust measured in a horizontal direction. This direction of measurement is important particularly in layered sedimentary rocks, in which the deformation modulus may be significantly different in different directions.

A plot of this equation is given in Figure 2 for a range of deformation moduli. The curves relating  $k$  with depth below surface  $z$  are similar to those published by Brown and Hoek (1978), Herget (1988) and others for measured in situ stresses. Hence equation 3 is considered to provide a reasonable basis for estimating the value of  $k$ .

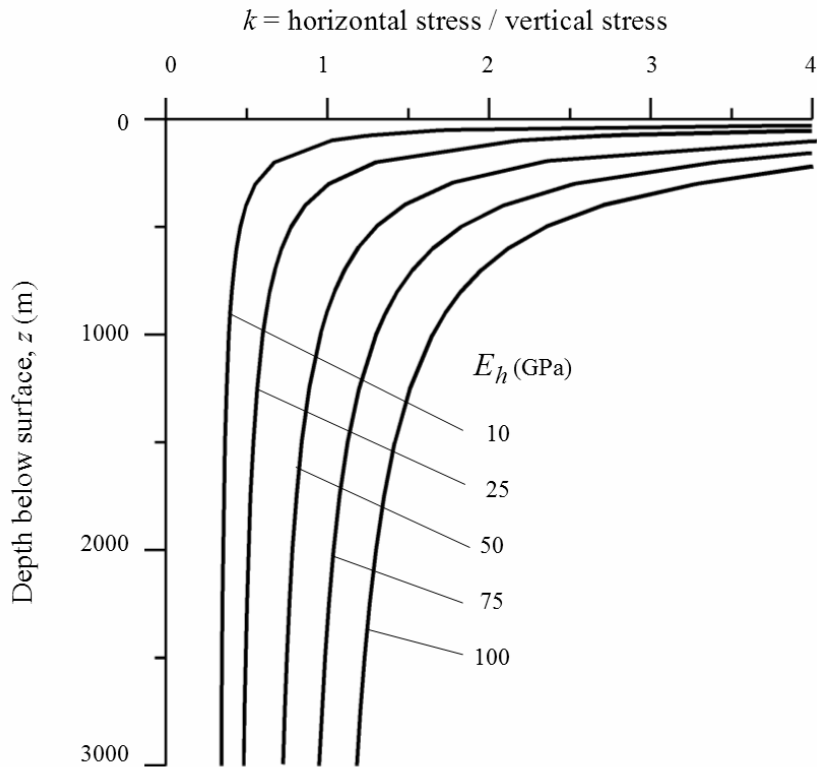


Figure 2: Ratio of horizontal to vertical stress for different deformation moduli based upon Sheorey's equation. (After Sheorey 1994).

### *In situ and induced stresses*

As pointed out by Sheorey, his work does not explain the occurrence of measured vertical stresses that are higher than the calculated overburden pressure, the presence of very high horizontal stresses at some locations or why the two horizontal stresses are seldom equal. These differences are probably due to local topographic and geological features that cannot be taken into account in a large scale model such as that proposed by Sheorey.

Where sensitivity studies have shown that the in situ stresses are likely to have a significant influence on the behaviour of underground openings, it is recommended that the in situ stresses should be measured. Suggestions for setting up a stress measuring programme are discussed later in this chapter.

#### **The World stress map**

The World Stress Map project, completed in July 1992, involved over 30 scientists from 18 countries and was carried out under the auspices of the International Lithosphere Project (Zoback, 1992). The aim of the project was to compile a global database of contemporary tectonic stress data.

The World Stress Map (WSM) is now maintained and it has been extended by the Geophysical Institute of Karlsruhe University as a research project of the Heidelberg Academy of Sciences and Humanities. The 2005 version of the map contains approximately 16,000 data sets and various versions of the map for the World, Europe, America, Africa, Asia and Australia can be downloaded from the Internet. The WSM is an open-access database that can be accessed at [www.world-stress-map.org](http://www.world-stress-map.org) (Reinecker et al, 2005)

The 2005 World Stress Map is reproduced in Figure 3 while a stress map for the Mediterranean is reproduced in Figure 4.

The stress maps display the orientations of the maximum horizontal compressive stress. The length of the stress symbols represents the data quality, with A being the best quality. Quality A data are assumed to record the orientation of the maximum horizontal compressive stress to within 10°-15°, quality B data to within 15°-20°, and quality C data to within 25°. Quality D data are considered to give questionable tectonic stress orientations.

The 1992 version of the World Stress Map was derived mainly from geological observations on earthquake focal mechanisms, volcanic alignments and fault slip interpretations. Less than 5% of the data was based upon hydraulic fracturing or overcoring measurements of the type commonly used in mining and civil engineering projects. In contrast, the 2005 version of the map includes a significantly greater number of observations from borehole break-outs, hydraulic fracturing, overcoring and borehole slotting. It is therefore worth considering the relative accuracy of these measurements as compared with the geological observations upon which the original map was based.

*In situ and induced stresses*

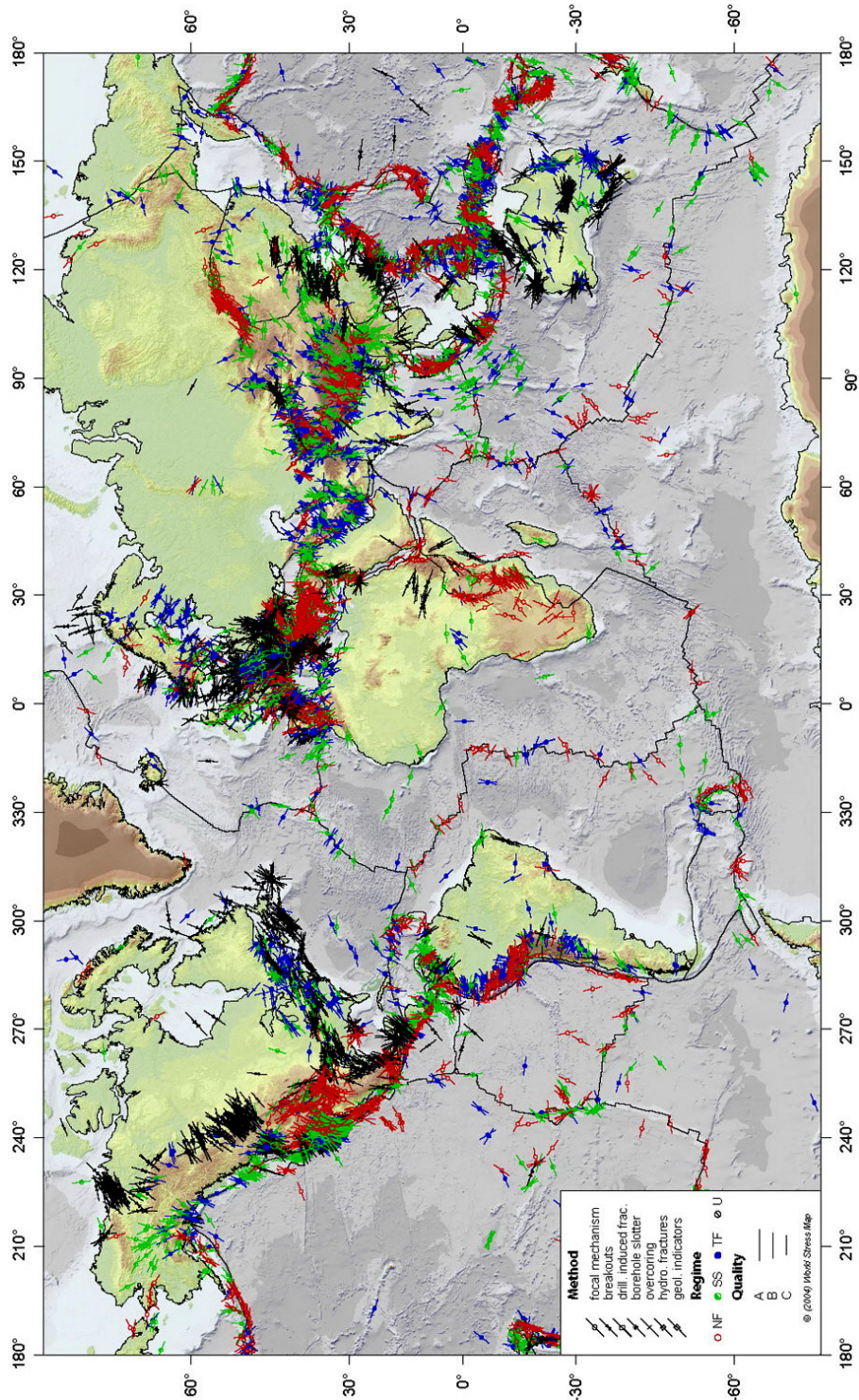


Figure 3: World stress map giving orientations of the maximum horizontal compressive stress. From [www.world-stress-map.org](http://www.world-stress-map.org).



*In situ and induced stresses*

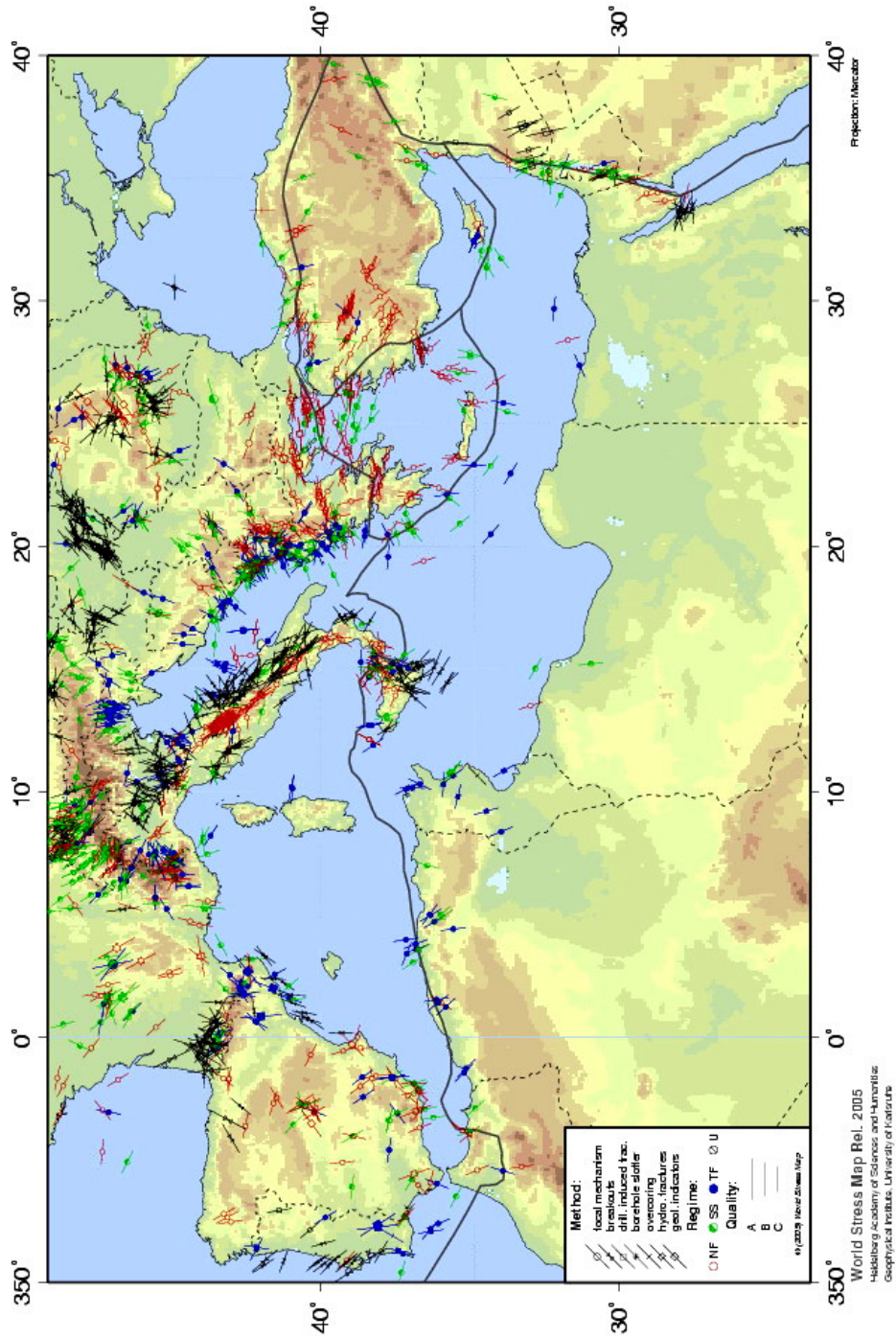


Figure 4: Stress map of the Mediterranean giving orientations of the maximum horizontal compressive stress. From [www.world-stress-map.org](http://www.world-stress-map.org).

### *In situ and induced stresses*

In discussing hydraulic fracturing and overcoring stress measurements, Zoback (1992) has the following comments:

‘Detailed hydraulic fracturing testing in a number of boreholes beginning very close to surface (10-20 m depth) has revealed marked changes in stress orientations and relative magnitudes with depth in the upper few hundred metres, possibly related to effects of nearby topography or a high degree of near surface fracturing.

Included in the category of ‘overcoring’ stress measurements are a variety of stress or strain relief measurement techniques. These techniques involve a three-dimensional measurement of the strain relief in a body of rock when isolated from the surrounding rock volume; the three-dimensional stress tensor can subsequently be calculated with a knowledge of the complete compliance tensor of the rock. There are two primary drawbacks with this technique which restricts its usefulness as a tectonic stress indicator: measurements must be made near a free surface, and strain relief is determined over very small areas (a few square millimetres to square centimetres). Furthermore, near surface measurements (by far the most common) have been shown to be subject to effects of local topography, rock anisotropy, and natural fracturing (Engelder and Sbar, 1984). In addition, many of these measurements have been made for specific engineering applications (e.g. dam site evaluation, mining work), places where topography, fracturing or nearby excavations could strongly perturb the regional stress field.’

Obviously, from a global or even a regional scale, the type of engineering stress measurements carried out in a mine or on a civil engineering site are not regarded as very reliable. Conversely, the World Stress Map versions presented in Figures 3 and 4 can only be used to give first order estimates of the stress directions which are likely to be encountered on a specific site. Since both stress directions and stress magnitudes are critically important in the design of underground excavations, it follows that a stress measuring programme may be required in any major underground mining or civil engineering project.

#### **Developing a stress measuring programme**

Consider the example of a tunnel to be driven a depth of 1,000 m below surface in a hard rock environment. The depth of the tunnel is such that it is probable that in situ and induced stresses will be an important consideration in the design of the excavation. Typical steps that could be followed in the analysis of this problem are:

The World Stress Map for the area under consideration will give a good first indication of the possible complexity of the regional stress field and possible directions for the maximum horizontal compressive stress.

### *In situ and induced stresses*

1. During preliminary design, the information presented in equations 1 and 3 can be used to obtain a first rough estimate of the vertical and average horizontal stress in the vicinity of the tunnel. For a depth of 1,000 m, these equations give the vertical stress  $\sigma_v = 27$  MPa, the ratio  $k = 1.3$  (for  $E_h = 75$  GPa) and hence the average horizontal stress  $\sigma_h = 35.1$  MPa. A preliminary analysis of the stresses induced around the proposed tunnel shows that these induced stresses are likely to exceed the strength of the rock and that the question of stress measurement must be considered in more detail. Note that for many openings in strong rock at shallow depth, stress problems may not be significant and the analysis need not proceed any further.

For this particular case, stress problems are considered to be important. A typical next step would be to search the literature in an effort to determine whether the results of in situ stress measurement programmes are available for mines or civil engineering projects within a radius of say 50 km of the site. With luck, a few stress measurement results will be available for the region in which the tunnel is located and these results can be used to refine the analysis discussed above.

Assuming that the results of the analysis of induced stresses in the rock surrounding the proposed tunnel indicate that significant zones of rock failure are likely to develop, and that support costs are likely to be high, it is probably justifiable to set up a stress measurement project on the site. These measurements can be carried out in deep boreholes from the surface, using hydraulic fracturing techniques, or from underground access using overcoring methods. The choice of the method and the number of measurements to be carried out depends upon the urgency of the problem, the availability of underground access and the costs involved in the project. Note that very few project organisations have access to the equipment required to carry out a stress measurement project and, rather than purchase this equipment, it may be worth bringing in an organisation which has the equipment and which specialises in such measurements.

2. Where regional tectonic features such as major faults are likely to be encountered the in situ stresses in the vicinity of the feature may be rotated with respect to the regional stress field. The stresses may be significantly different in magnitude from the values estimated from the general trends described above. These differences can be very important in the design of the openings and in the selection of support and, where it is suspected that this is likely to be the case, in situ stress measurements become an essential component of the overall design process.

### **Analysis of induced stresses**

When an underground opening is excavated into a stressed rock mass, the stresses in the vicinity of the new opening are re-distributed. Consider the example of the stresses induced in the rock surrounding a horizontal circular tunnel as illustrated in Figure 5, showing a vertical slice normal to the tunnel axis.

### *In situ and induced stresses*

Before the tunnel is excavated, the in situ stresses  $\sigma_v$ ,  $\sigma_{h1}$  and  $\sigma_{h2}$  are uniformly distributed in the slice of rock under consideration. After removal of the rock from within the tunnel, the stresses in the immediate vicinity of the tunnel are changed and new stresses are induced. Three principal stresses  $\sigma_1$ ,  $\sigma_2$  and  $\sigma_3$  acting on a typical element of rock are shown in Figure 5.

The convention used in rock engineering is that *compressive* stresses are always *positive* and the three principal stresses are numbered such that  $\sigma_1$  is the largest compressive stress and  $\sigma_3$  is the smallest compressive stress or the largest tensile stress of the three.

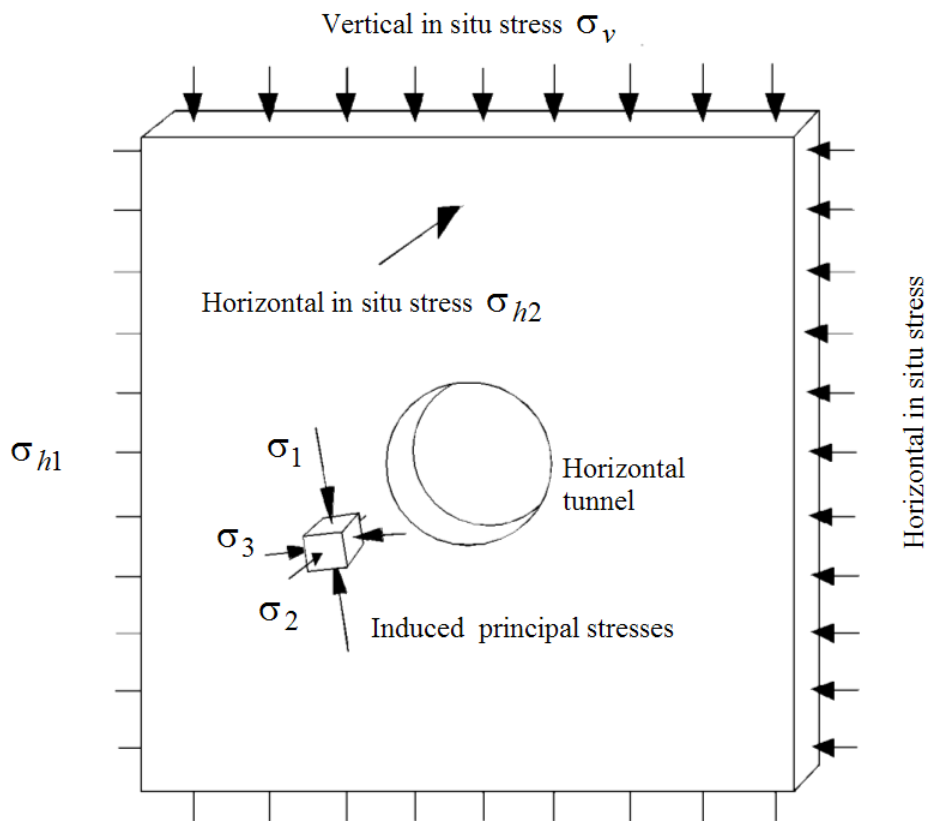


Figure 5: Illustration of principal stresses induced in an element of rock close to a horizontal tunnel subjected to a vertical in situ stress  $\sigma_v$ , a horizontal in situ stress  $\sigma_{h1}$  in a plane normal to the tunnel axis and a horizontal in situ stress  $\sigma_{h2}$  parallel to the tunnel axis.

*In situ and induced stresses*

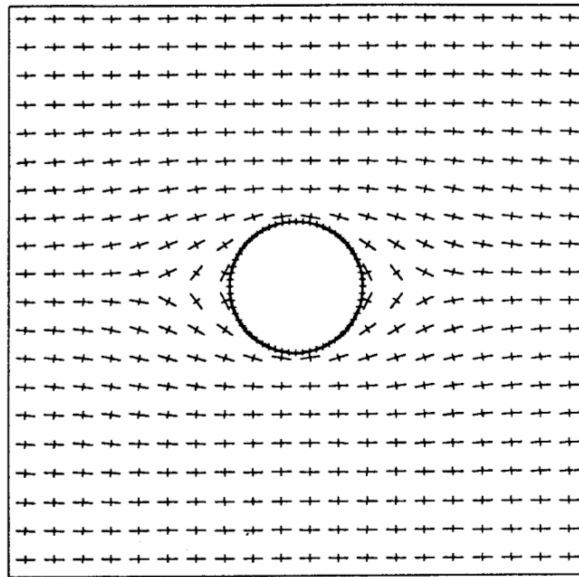


Figure 6: Principal stress directions in the rock surrounding a horizontal tunnel subjected to a horizontal in situ stress  $\sigma_{h1}$  equal to  $3\sigma_v$ , where  $\sigma_v$  is the vertical in situ stress.

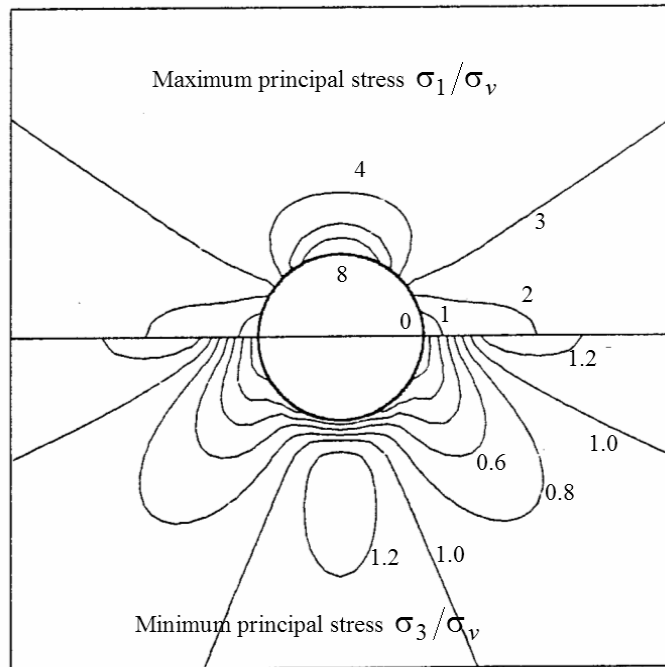


Figure 7: Contours of maximum and minimum principal stress magnitudes in the rock surrounding a horizontal tunnel, subjected to a vertical in situ stress of  $\sigma_v$  and a horizontal in situ stress of  $3\sigma_v$ .

### *In situ and induced stresses*

The three principal stresses are mutually perpendicular but they may be inclined to the direction of the applied in situ stress. This is evident in Figure 6 which shows the directions of the stresses in the rock surrounding a horizontal tunnel subjected to a horizontal in situ stress  $\sigma_{h1}$  equal to three times the vertical in situ stress  $\sigma_v$ . The longer bars in this figure represent the directions of the maximum principal stress  $\sigma_1$ , while the shorter bars give the directions of the minimum principal stress  $\sigma_3$  at each element considered. In this particular case,  $\sigma_2$  is coaxial with the in situ stress  $\sigma_{h2}$ , but the other principal stresses  $\sigma_1$  and  $\sigma_3$  are inclined to  $\sigma_{h1}$  and  $\sigma_v$  in the immediate vicinity of the tunnel.

Contours of the magnitudes of the maximum principal stress  $\sigma_1$  and the minimum principal stress  $\sigma_3$  are given in Figure 7. This figure shows that the redistribution of stresses is concentrated in the rock close to the tunnel and that, at a distance of say three times the radius from the centre of the hole, the disturbance to the in situ stress field is negligible.

An analytical solution for the stress distribution in a stressed elastic plate containing a circular hole was published by Kirsch (1898) and this formed the basis for many early studies of rock behaviour around tunnels and shafts. Following along the path pioneered by Kirsch, researchers such as Love (1927), Muskhelishvili (1953) and Savin (1961) published solutions for excavations of various shapes in elastic plates. A useful summary of these solutions and their application in rock mechanics was published by Brown in an introduction to a volume entitled *Analytical and Computational Methods in Engineering Rock Mechanics* (1987).

Closed form solutions still possess great value for conceptual understanding of behaviour and for the testing and calibration of numerical models. For design purposes, however, these models are restricted to very simple geometries and material models. They are of limited practical value. Fortunately, with the development of computers, many powerful programs that provide numerical solutions to these problems are now readily available. A brief review of some of these numerical solutions is given below.

#### **Numerical methods of stress analysis**

Most underground excavations are irregular in shape and are frequently grouped close to other excavations. These groups of excavations can form a set of complex three-dimensional shapes. In addition, because of the presence of geological features such as faults and dykes, the rock properties are seldom uniform within the rock volume of interest. Consequently, closed form solutions are of limited value in calculating the stresses, displacements and failure of the rock mass surrounding underground excavations. A number of computer-based numerical methods have been developed over the past few decades and these methods provide the means for obtaining approximate solutions to these problems.

### *In situ and induced stresses*

Numerical methods for the analysis of stress driven problems in rock mechanics can be divided into two classes:

- *Boundary discretization methods*, in which only the boundary of the excavation is divided into elements and the interior of the rock mass is represented mathematically as an infinite continuum. These methods are normally restricted to elastic analyses.
- *Domain discretization methods*, in which the interior of the rock mass is divided into geometrically simple elements each with assumed properties. The collective behaviour and interaction of these simplified elements model the more complex overall behaviour of the rock mass. In other words domain methods allow consideration of more complex material models than boundary methods. *Finite element* and *finite difference* methods are domain techniques which treat the rock mass as a continuum. The *distinct element* method is also a domain method which models each individual block of rock as a unique element.

These two classes of analysis can be combined in the form of *hybrid models* in order to maximise the advantages and minimise the disadvantages of each method.

It is possible to make some general observations about the two types of approaches discussed above. In domain methods, a significant amount of effort is required to create the mesh that is used to divide the rock mass into elements. In the case of complex models, such as those containing multiple openings, meshing can become extremely difficult. In contrast, boundary methods require only that the excavation boundary be discretized and the surrounding rock mass is treated as an infinite continuum. Since fewer elements are required in the boundary method, the demand on computer memory and on the skill and experience of the user is reduced. The availability of highly optimised mesh-generators in many domain models has narrowed this difference to the point where most users of domain programs would be unaware of the mesh generation problems discussed above and hence the choice of models can be based on other considerations.

In the case of domain methods, the outer boundaries of the model must be placed sufficiently far away from the excavations in order that errors, arising from the interaction between these outer boundaries and the excavations, are reduced to an acceptable minimum. On the other hand, since boundary methods treat the rock mass as an infinite continuum, the far field conditions need only be specified as stresses acting on the entire rock mass and no outer boundaries are required. The main strength of boundary methods lies in the simplicity achieved by representing the rock mass as a continuum of infinite extent. It is this representation, however, that makes it difficult to incorporate variable material properties and discontinuities such as joints and faults. While techniques have been developed to allow some boundary element modelling of variable rock properties, these types of problems are more conveniently modelled by domain methods.

## *In situ and induced stresses*

Before selecting the appropriate modelling technique for particular types of problems, it is necessary to understand the basic components of each technique.

### *Boundary Element Method*

The boundary element method derives its name from the fact that only the boundaries of the problem geometry are divided into elements. In other words, only the excavation surfaces, the free surface for shallow problems, joint surfaces where joints are considered explicitly and material interfaces for multi-material problems are divided into elements. In fact, several types of boundary element models are collectively referred to as 'the boundary element method' (Crouch and Starfield, 1983). These models may be grouped as follows:

*Indirect (Fictitious Stress) method*, so named because the first step in the solution is to find a set of fictitious stresses that satisfy prescribed boundary conditions. These stresses are then used in the calculation of actual stresses and displacements in the rock mass.

*Direct method*, so named because the displacements are solved directly for the specified boundary conditions.

*Displacement Discontinuity method*, so named because the solution is based on the superposition of the fundamental solution of an elongated slit in an elastic continuum and shearing and normal displacements in the direction of the slit.

The differences between the first two methods are not apparent to the program user. The direct method has certain advantages in terms of program development, as will be discussed later in the section on Hybrid approaches.

The fact that a boundary element model extends 'to infinity' can also be a disadvantage. For example, a heterogeneous rock mass consists of regions of finite, not infinite, extent. Special techniques must be used to handle these situations. Joints are modelled explicitly in the boundary element method using the displacement discontinuity approach, but this can result in a considerable increase in computational effort. Numerical convergence is often found to be a problem for models incorporating many joints. For these reasons, problems, requiring explicit consideration of several joints and/or sophisticated modelling of joint constitutive behaviour, are often better handled by one of the domain methods such as finite elements.

A widely-used application of displacement discontinuity boundary elements is in the modelling of tabular ore bodies. Here, the entire ore seam is represented as a 'discontinuity' which is initially filled with ore. Mining is simulated by reduction of the ore stiffness to zero in those areas where mining has occurred, and the resulting stress redistribution to the surrounding pillars may be examined (Salamon, 1974, von Kimmelman et al., 1984).



*Finite element and finite difference methods*

In practice, the finite element method is usually indistinguishable from the finite difference method; thus, they will be treated here as one and the same. For the boundary element method, it was seen that conditions on a domain boundary could be related to the state at *all* points throughout the remaining rock, even to infinity. In comparison, the finite element method relates the conditions at a few points within the rock (nodal points) to the state within a finite closed region formed by these points (the element). In the finite element method the physical problem is modelled numerically by dividing the entire problem region into elements.

The finite element method is well suited to solving problems involving heterogeneous or non-linear material properties, since each element explicitly models the response of its contained material. However, finite elements are not well suited to modelling infinite boundaries, such as occur in underground excavation problems. One technique for handling infinite boundaries is to discretize beyond the zone of influence of the excavation and to apply appropriate boundary conditions to the outer edges. Another approach has been to develop elements for which one edge extends to infinity i.e. so-called 'infinity' finite elements. In practice, efficient pre- and post-processors allow the user to perform parametric analyses and assess the influence of approximated far-field boundary conditions. The time required for this process is negligible compared to the total analysis time.

Joints can be represented explicitly using specific 'joint elements'. Different techniques have been proposed for handling such elements, but no single technique has found universal favour. Joint interfaces may be modelled, using quite general constitutive relations, though possibly at increased computational expense depending on the solution technique.

Once the model has been divided into elements, material properties have been assigned and loads have been prescribed, some technique must be used to redistribute any unbalanced loads and thus determine the solution to the new equilibrium state. Available solution techniques can be broadly divided into two classes - implicit and explicit. Implicit techniques assemble systems of linear equations that are then solved using standard matrix reduction techniques. Any material non-linearity is accounted for by modifying stiffness coefficients (secant approach) and/or by adjusting prescribed variables (initial stress or initial strain approach). These changes are made in an iterative manner such that all constitutive and equilibrium equations are satisfied for the given load state.

The response of a non-linear system generally depends upon the sequence of loading. Thus it is necessary that the load path modelled be representative of the actual load path experienced by the body. This is achieved by breaking the total applied load into load increments, each increment being sufficiently small, so that solution convergence for the increment is achieved after only a few iterations. However, as the system being modelled becomes increasingly non-linear and the load increment

### *In situ and induced stresses*

represents an ever smaller portion of the total load, the incremental solution technique becomes similar to modelling the quasi-dynamic behaviour of the body, as it responds to gradual application of the total load.

In order to overcome this, a 'dynamic relaxation' solution technique was proposed (Otter et al., 1966) and first applied to geomechanics modelling by Cundall (1971). In this technique no matrices are formed. Rather, the solution proceeds explicitly - unbalanced forces, acting at a material integration point, result in acceleration of the mass associated with the point; applying Newton's law of motion expressed as a difference equation yields incremental displacements, applying the appropriate constitutive relation produces the new set of forces, and so on marching in time, for each material integration point in the model. This solution technique has the advantage that both geometric and material non-linearities are accommodated, with relatively little additional computational effort as compared to a corresponding linear analysis, and computational expense increases only linearly with the number of elements used. A further practical advantage lies in the fact that numerical divergence usually results in the model predicting obviously anomalous physical behaviour. Thus, even relatively inexperienced users may recognise numerical divergence.

Most commercially available finite element packages use implicit (i.e. matrix) solution techniques. For linear problems and problems of moderate non-linearity, implicit techniques tend to perform faster than explicit solution techniques. However, as the degree of non-linearity of the system increases, imposed loads must be applied in smaller increments which implies a greater number of matrix re-formations and reductions, and hence increased computational expense. Therefore, highly non-linear problems are best handled by packages using an explicit solution technique.

#### *Distinct Element Method*

In ground conditions conventionally described as blocky (i.e. where the spacing of the joints is of the same order of magnitude as the excavation dimensions), intersecting joints form wedges of rock that may be regarded as rigid bodies. That is, these individual pieces of rock may be free to rotate and translate, and the deformation that takes place at block contacts may be significantly greater than the deformation of the intact rock. Hence, individual wedges may be considered rigid. For such conditions it is usually necessary to model many joints explicitly. However, the behaviour of such systems is so highly non-linear, that even a jointed finite element code, employing an explicit solution technique, may perform relatively inefficiently.

An alternative modelling approach is to develop data structures that represent the blocky nature of the system being analysed. Each block is considered a unique free body that may interact at contact locations with surrounding blocks. Contacts may be represented by the overlaps of adjacent blocks, thereby avoiding the necessity of unique joint elements. This has the added advantage that arbitrarily large relative displacements at the contact may occur, a situation not generally tractable in finite element codes.

### *In situ and induced stresses*

Due to the high degree of non-linearity of the systems being modelled, explicit solution techniques are favoured for distinct element codes. As is the case for finite element codes employing explicit solution techniques, this permits very general constitutive modelling of joint behaviour with little increase in computational effort and results in computation time being only linearly dependent on the number of elements used. The use of explicit solution techniques places fewer demands on the skills and experience than the use of codes employing implicit solution techniques.

Although the distinct element method has been used most extensively in academic environments to date, it is finding its way into the offices of consultants, planners and designers. Further experience in the application of this powerful modelling tool to practical design situations and subsequent documentation of these case histories is required, so that an understanding may be developed of where, when and how the distinct element method is best applied.

### *Hybrid approaches*

The objective of a hybrid method is to combine the above methods in order to eliminate undesirable characteristics while retaining as many advantages as possible. For example, in modelling an underground excavation, most non-linearity will occur close to the excavation boundary, while the rock mass at some distance will behave in an elastic fashion. Thus, the near-field rock mass might be modelled, using a distinct element or finite element method, which is then linked at its outer limits to a boundary element model, so that the far-field boundary conditions are modelled exactly. In such an approach, the direct boundary element technique is favoured as it results in increased programming and solution efficiency.

Lorig and Brady (1984) used a hybrid model consisting of a discrete element model for the near field and a boundary element model for the far field in a rock mass surrounding a circular tunnel.

### *Two-dimensional and three-dimensional models*

A two-dimensional model, such as that illustrated in Figure 5, can be used for the analysis of stresses and displacements in the rock surrounding a tunnel, shaft or borehole, where the length of the opening is much larger than its cross-sectional dimensions. The stresses and displacements in a plane, normal to the axis of the opening, are not influenced by the ends of the opening, provided that these ends are far enough away.

On the other hand, an underground powerhouse or crusher chamber has a much more equi-dimensional shape and the effect of the end walls cannot be neglected. In this case, it is much more appropriate to carry out a three-dimensional analysis of the stresses and displacements in the surrounding rock mass. Unfortunately, this switch from two to three dimensions is not as simple as it sounds and there are relatively few

### *In situ and induced stresses*

good three-dimensional numerical models, which are suitable for routine stress analysis work in a typical engineering design office.

EXAMINE3D ([www.roscience.com](http://www.roscience.com)) is a three-dimensional boundary element program that provides a starting point for an analysis of a problem in which the three-dimensional geometry of the openings is important. Such three-dimensional analyses provide clear indications of stress concentrations and of the influence of three-dimensional geometry. In many cases, it is possible to simplify the problem to two-dimensions by considering the stresses on critical sections identified in the three-dimensional model.

More sophisticated three-dimensional finite element models such as FLAC3D ([www.itascacg.com](http://www.itascacg.com)) are available, but the definition of the input parameters and interpretation of the results of these models would stretch the capabilities of all but the most experienced modellers. It is probably best to leave this type of modelling in the hands of these specialists.

It is recommended that, where the problem being considered is obviously three-dimensional, a preliminary elastic analysis be carried out by means of one of the three-dimensional boundary element programs. The results can then be used to decide whether further three-dimensional analyses are required or whether appropriate two-dimensional sections can be modelled using a program such as PHASE2 ([www.roscience.com](http://www.roscience.com)), a powerful but user-friendly finite element program that generally meets the needs of most underground excavation design projects.

#### **Examples of two-dimensional stress analysis**

A boundary element program called EXAMINE2D is available as a free download from [www.roscience.com](http://www.roscience.com). While this program is limited to elastic analyses it can provide a very useful introduction for those who are not familiar with the numerical stress analysis methods described above. The following examples demonstrate the use of this program to explore some common problems in tunnelling.

##### *Tunnel shape*

Most contractors like a simple horseshoe shape for tunnels since this gives a wide flat floor for the equipment used during construction. For relatively shallow tunnels in good quality rock this is an appropriate tunnel shape and there are many hundreds of kilometres of horseshoe shaped tunnels all over the world.

In poor quality rock masses or in tunnels at great depth, the simple horseshoe shape is not a good choice because of the high stress concentrations at the corners where the sidewalls meet the floor or invert. In some cases failures initiating at these corners can lead to severe floor heave and even to failure of the entire tunnel perimeter as shown in Figure 8.



Figure 8: Failure of the lining in a horseshoe shaped tunnel in a highly stressed poor quality rock mass. This failure initiated at the corners where the invert meets the sidewalls.

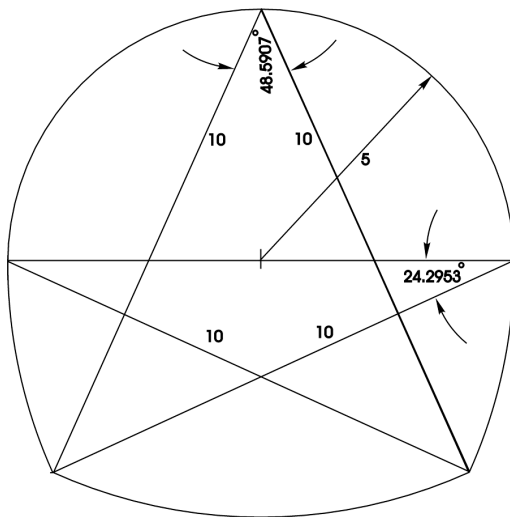
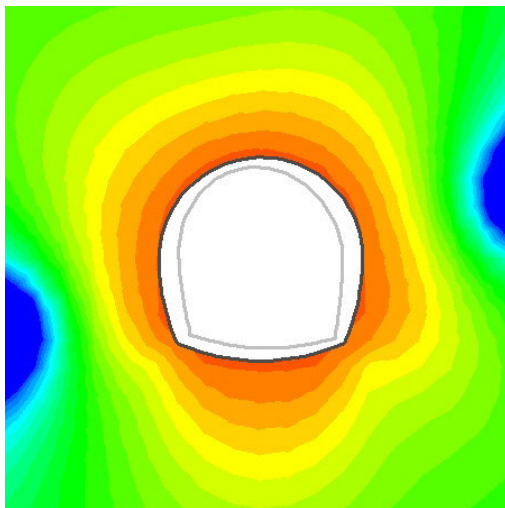
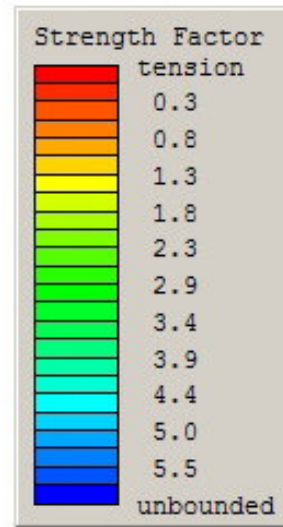
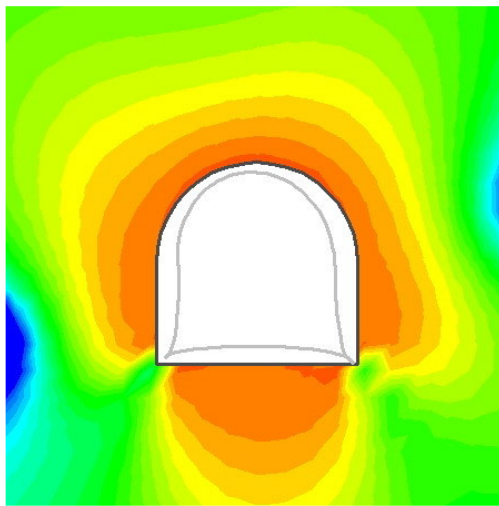


Figure 9: Dimensions of a 10 m span modified horseshoe tunnel shape designed to overcome some of the problems illustrated in Figure 8.

The stress distribution in the rock mass surrounding the tunnel can be improved by modifying the horseshoe shape as shown in Figure 9. In some cases this can eliminate or minimise the types of failure shown in Figure 8 while, in other cases, it may be necessary to use a circular tunnel profile.

*In situ and induced stresses*



In situ stresses:

Major principal stress  $\sigma_1 = 10$  MPa  
 Minor principal stress  $\sigma_3 = 7$  MPa  
 Intermediate principal stress  $\sigma_2 = 9$  MPa  
 Inclination of major principal stress to the horizontal axis =  $15^\circ$

Rock mass properties:

Friction angle  $\phi = 35^\circ$   
 Cohesion  $c = 1$  MPa  
 Tensile strength = zero  
 Deformation modulus  $E = 4600$  MPa

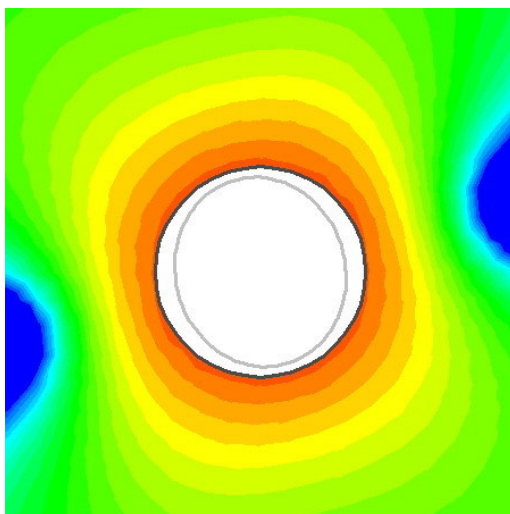


Figure 10: Comparison of three tunnel excavation profiles using EXAMINE2D. The contours are for the Strength Factor defined by the ratio of rock mass strength to the induced stress at each point. The deformed boundary profile (exaggerated) is shown inside each excavation.

### *In situ and induced stresses*

The application of the program EXAMINE2D to compare three tunnel shapes is illustrated in Figure 10. Typical “average” in situ stresses and rock mass properties were used in this analysis and the three figures compare Strength Factor contours and deformed excavation profiles (exaggerated) for the three tunnel shapes.

It is clear that the flat floor of the horseshoe tunnel (top figure) allows upward displacement or heaving of the floor. The sharp corners at the junction between the floor and the tunnel sidewalls create high stress concentrations and also generate large bending moments in any lining installed in the tunnel. Failure of the floor generally initiates at these corners as illustrated in Figure 8.

Floor heave is reduced significantly by the concave curvature of the floor of the modified horseshoe shape (middle figure). In marginal cases these modifications to the horseshoe shape may be sufficient to prevent or at least minimise the type of damage illustrated in Figure 8. However, in severe cases, a circular tunnel profile is invariably the best choice, as shown by the smooth Strength Factor contours and the deformed tunnel boundary shape in the bottom figure in Figure 10.

### *Large underground caverns*

A typical underground complex in a hydroelectric project has a powerhouse with a span of 20 to 25 m and a height of 40 to 50 m. Four to six turbine-generator sets are housed in this cavern and a cutaway sketch through one of these sets is shown in Figure 11. Transformers are frequently housed in a chamber or gallery parallel to the powerhouse. Ideally these two caverns should be as close as possible in order to minimise the length of the bus-bars connecting the generators and transformers. This has to be balanced against the size and hence the stability of the pillar between the caverns. The relative location and distance between the caverns is explored in the series of EXAMINE2D models shown in Figure 12, using the same in situ stresses and rock mass properties as listed in Figure 10.

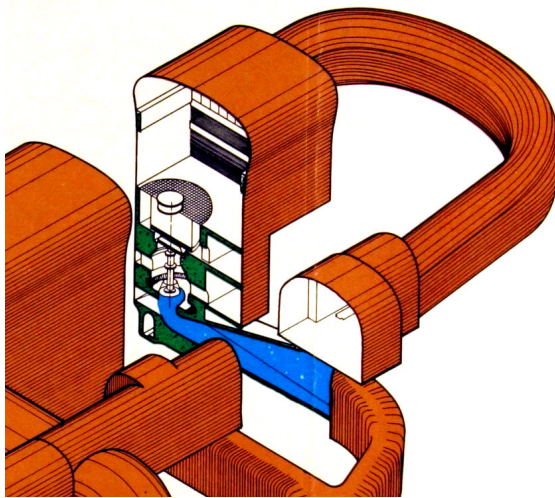
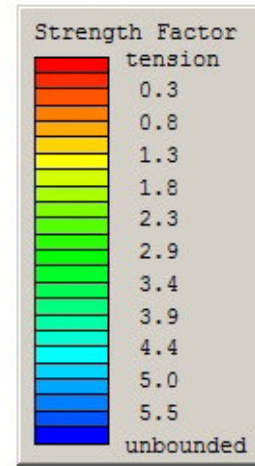
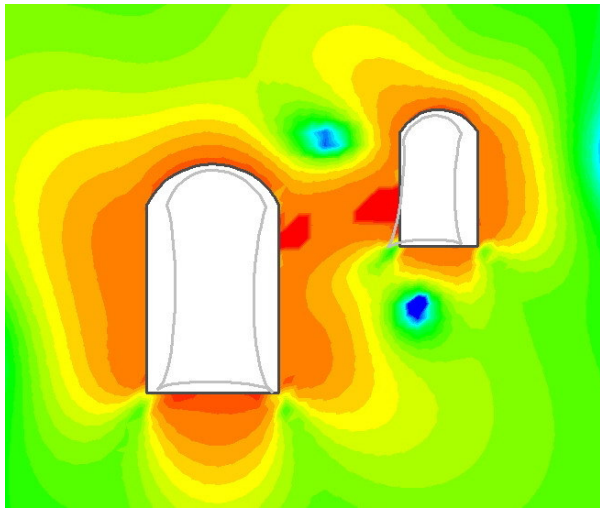


Figure 11: Cutaway sketch of the layout of an underground powerhouse cavern and a parallel transformer gallery.

*In situ and induced stresses*



In situ stresses:

Major principal stress  $\sigma_1 = 10$  MPa  
Minor principal stress  $\sigma_3 = 7$  MPa  
Intermediate stress  $\sigma_2 = 9$  MPa  
Inclination of major principal stress to the horizontal axis =  $15^\circ$

Rock mass properties:

Friction angle  $\phi = 35^\circ$   
Cohesion  $c = 1$  MPa  
Tensile strength = zero  
Deformation modulus  $E = 4600$  MPa

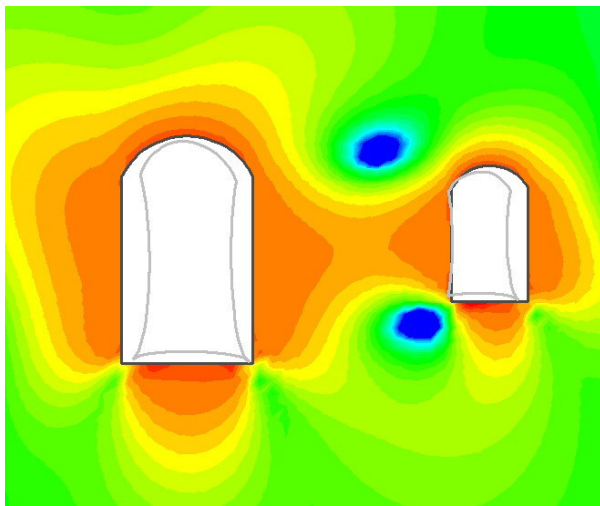
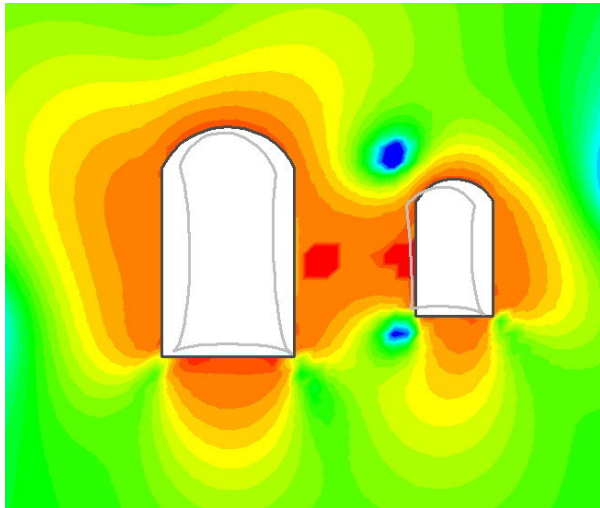


Figure 12: Comparison of three underground powerhouse and transformer gallery layouts, using EXAMINE2D. The contours are for the Strength Factor defined by the ratio of rock mass strength to the induced stress at each point. The deformed boundary profile (exaggerated) is shown inside each excavation.



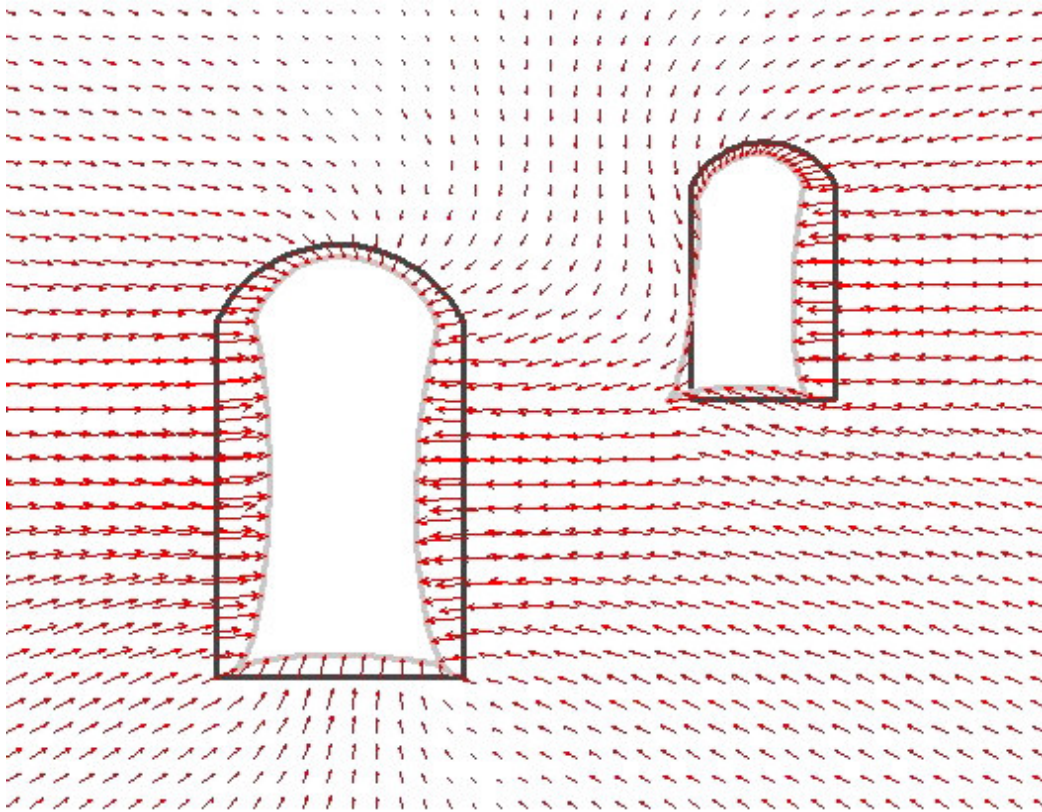


Figure 13: Displacement vectors and deformed excavation shapes for the underground powerhouse and transformer gallery.

A closer examination of the deformations induced in the rock mass by the excavation of the underground powerhouse and transformer gallery, in Figure 13, shows that the smaller of the two excavations is drawn towards the larger cavern and its profile is distorted in this process. This distortion can be reduced by relocating the transformer gallery and by increasing the spacing between the galleries as has been done in Figure 12.

Where the combination of rock mass strength and in situ stresses is likely to cause overstressing around the caverns and in the pillar, a good rule of thumb is that the distance between the two caverns should be approximately equal to the height of the larger cavern.

The interested reader is encouraged to download the program EXAMINE2D (free from [www.rocsscience.com](http://www.rocsscience.com)) and to use it to explore the problem, such as those illustrated in Figures 10 and 12, for themselves.

## References

- Brown, E.T. 1987. Introduction. *Analytical and computational methods in engineering rock mechanics*, (ed. E.T. Brown), 1-31. London: Allen and Unwin.
- Brown, E.T. and Hoek, E. 1978. Trends in relationships between measured rock in situ stresses and depth. *Int. J. Rock Mech. Min. Sci. & Geomech. Abstr.* **15**, pp.211-215.
- Crouch, S.L. and Starfield, A.M. 1983. *Boundary element methods in solid mechanics*. London: Allen and Unwin.
- Cundall, P.A. 1971. A computer model for simulating progressive large scale movements in blocky rock systems. In *Rock Fracture, Proc. symp. ISRM, Nancy 1*, Paper 2-8.
- Engelder, T. and Sbar, M.L. 1984. Near-surface in situ stress: introduction. *J. Geophys. Res.* **89**, pp.9321-9322. Princeton, NJ: Princeton University Press.
- Herget, G. 1988. *Stresses in rock*. Rotterdam: Balkema.
- Hoek, E., Carranza – Torres, C. and Corkum, B., 2002. Hoek - Brown failure criterion – 2002 edition. In *Proceedings of NARMS-TAC 2002*, Toronto (eds. Bawden, R.W., Curran, J., Telesnicki, M) pp. 267-273. Download from [www.roscience.com](http://www.roscience.com)
- Kirsch, G., 1898. Die theorie der elastizitat und die bedurfnisse der festigkeitslehre. *Veit. Deit. Ing.* **42** (28), 797-807.
- Lorig, L.J. and Brady, B.H.G. 1984. A hybrid computational scheme for excavation and support design in jointed rock media. In *Design and performance of underground excavations*, (eds E.T. Brown and J.A. Hudson), 105-112. London: Brit. Geotech. Soc.
- Love, A.E.H. 1927. A treatise on the mathematical theory of elasticity. New York: Dover.
- Muskhelishvili, N.I. 1953. *Some basic problems of the mathematical theory of elasticity*. 4th edn, translated by J.R.M. Radok. Gronigen: Noordhoff.
- Otter, J.R.H., Cassell, A.C. and Hobbs, R.E. 1966. Dynamic relaxation. *Proc. Instn Civ. Engrs* **35**, 633-665.
- Reinecker, J., Heidbach, O., Tingay, M., Sperner, B., & Müller, B. 2005: The release 2005 of the World Stress Map (available online at [www.world-stress-map.org](http://www.world-stress-map.org)).
- Salamon, M.D.G. 1974. Rock mechanics of underground excavations. In *Advances in rock mechanics, Proc. 3rd Cong. ISRM., Denver 1B*, 951-1009. Washington, DC: National Academy of Sciences
- Savin, G.N. 1961. *Stress concentrations around holes*. London: Pergamon.
- Sheory, P.R. 1994. A theory for in situ stresses in isotropic and transversely isotropic rock. *Int. J. Rock Mech. Min. Sci. & Geomech. Abstr.* **31**(1), 23-34.
- Terzaghi, K. and Richart, F.E. 1952. Stresses in rock about cavities. *Geotechnique* **3**, 57-90.

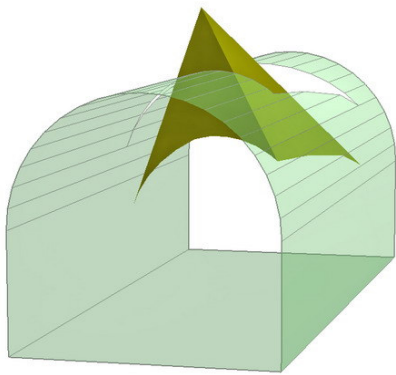
*In situ and induced stresses*

- von Kimmelman, M.R., Hyde, B. and Madgwick, R.J. 1984. The use of computer applications at BCL Limited in planning pillar extraction and the design of mine layouts. In *Design and performance of underground excavations*, (eds E.T. Brown and J.A. Hudson), 53-64. London: Brit. Geotech. Soc.
- Zoback, M. L. 1992. First- and second-order patterns of stress in the lithosphere: the World Stress Map Project. *J. Geophys. Res.* **97**(B8), 11761-11782.

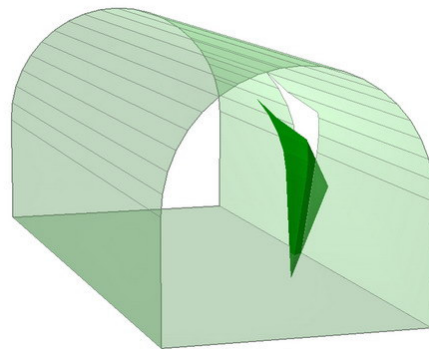
# Structurally controlled instability in tunnels

## Introduction

In tunnels excavated in jointed rock masses at relatively shallow depth, the most common types of failure are those involving wedges falling from the roof or sliding out of the sidewalls of the openings. These wedges are formed by intersecting structural features, such as bedding planes and joints, which separate the rock mass into discrete but interlocked pieces. When a free face is created by the excavation of the opening, the restraint from the surrounding rock is removed. One or more of these wedges can fall or slide from the surface if the bounding planes are continuous or rock bridges along the discontinuities are broken.



Roof fall



Sidewall wedge

Unless steps are taken to support these loose wedges, the stability of the back and walls of the opening may deteriorate rapidly. Each wedge, which is allowed to fall or slide, will cause a reduction in the restraint and the interlocking of the rock mass and this, in turn, will allow other wedges to fall. This failure process will continue until natural arching in the rock mass prevents further unravelling or until the opening is full of fallen material.

The steps which are required to deal with this problem are:

1. Determination of average dip and dip direction of significant discontinuity sets.
2. Identification of potential wedges which can slide or fall from the back or walls.
3. Calculation of the factor of safety of these wedges, depending upon the mode of failure.
4. Calculation of the amount of reinforcement required to bring the factor of safety of individual wedges up to an acceptable level.

### Identification of potential wedges

The size and shape of potential wedges in the rock mass surrounding an opening depends upon the size, shape and orientation of the opening and also upon the orientation of the significant discontinuity sets. The three-dimensional geometry of the problem necessitates a set of relatively tedious calculations. While these can be performed by hand, it is far more efficient to utilise one of the computer programs which are available. One such program, called UNWEDGE<sup>1</sup>, was developed specifically for use in underground hard rock mining and is utilised in the following discussion.

Consider a rock mass in which three strongly developed joint sets occur. The average dips and dip directions of these sets, shown as great circles in Figure 1, are as follows:

<i>Joint set</i>	<i>dip</i> <sup>o</sup>	<i>dip direction</i> <sup>o</sup>
J1	70 ± 5	036 ± 12
J2	85 ± 8	144 ± 10
J3	55 ± 6	262 ± 15

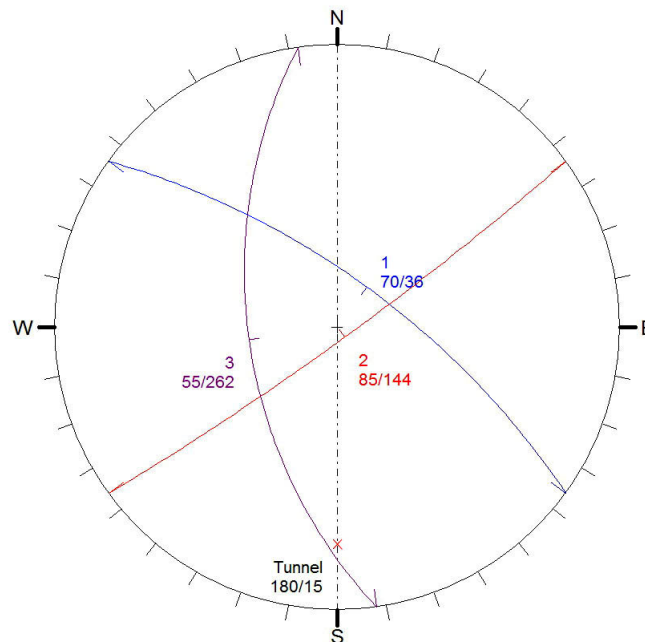
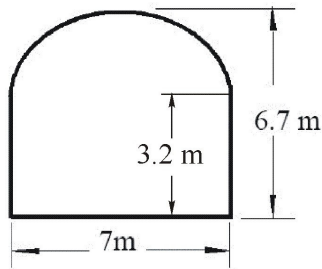


Figure 1: An equal area lower hemisphere plot of great circles representing the average dip and dip directions of three discontinuity sets in a rock mass. Also shown, as a chain dotted line, is the trend of the axis of a tunnel excavated in this rock mass. The tunnel plunge is marked with a red cross.

<sup>1</sup> Available from [www.rocscience.com](http://www.rocscience.com).

### *Structurally controlled stability in tunnels*

It is assumed that all of these discontinuities are planar and continuous and that the shear strength of the surfaces can be represented by a friction angle  $\phi = 30^\circ$  and a cohesive strength of zero. These shear strength properties are very conservative estimates, but they provide a reasonable starting point for most analyses of this type.



Tunnel section

A tunnel is to be excavated in this rock mass and the cross-section of the ramp is given in the sketch. The axis of the tunnel is inclined at  $15^\circ$  to the horizontal or, to use the terminology associated with structural geology analysis, the tunnel axis plunges at  $15^\circ$ . In the portion of the tunnel under consideration in this example, the axis runs due north-south or the trend of the axis is  $180^\circ$ .

The tunnel axis is shown as a chain dotted line in the stereonet in Figure 1. The trend of the axis is shown as  $0^\circ$ , measured clockwise from north. The plunge of the axis is  $15^\circ$  and this is shown as a cross on the chain dotted line representing the axis. The angle is measured inwards from the perimeter of the stereonet since this perimeter represents a horizontal reference plane.

The three structural discontinuity sets, represented by the great circles plotted in Figure 1, are entered into the program UNWEDGE, together with the cross-section of the tunnel and the plunge and trend of the tunnel axis. The program then determines the location and dimensions of the largest wedges which can be formed in the roof, floor and sidewalls of the excavation as shown in Figure 2.

The maximum number of simple tetrahedral wedges which can be formed by three discontinuities in the rock mass surrounding a circular tunnel is 6. In the case of a square or rectangular tunnel this number is reduced to 4. For the tunnel under consideration in this example, four wedges are formed.

Note that these wedges are the largest wedges which can be formed for the given geometrical conditions. The calculation used to determine these wedges assumes that the discontinuities are ubiquitous, in other words, they can occur anywhere in the rock mass. The joints, bedding planes and other structural features included in the analysis are also assumed to be planar and continuous. These conditions mean that the analysis will always find the largest possible wedges which can form. This result can generally be considered conservative since the size of wedges, formed in actual rock masses, will be limited by the persistence and the spacing of the structural features. The program UNWEDGE allows wedges to be scaled down to more realistic sizes if it is considered that maximum wedges are unlikely to form.

*Structurally controlled stability in tunnels*

Details of the four wedges illustrated in Figure 2 are given in the following table:

Wedge	Weight - tonnes	Failure mode	Factor of Safety
Roof wedge	44.2	Falls	0
Right side wedge	5.2	Slides on J1/J2	0.36
Left side wedge	3.6	Slides on J3	0.40
Floor wedge	182	Stable	$\infty$

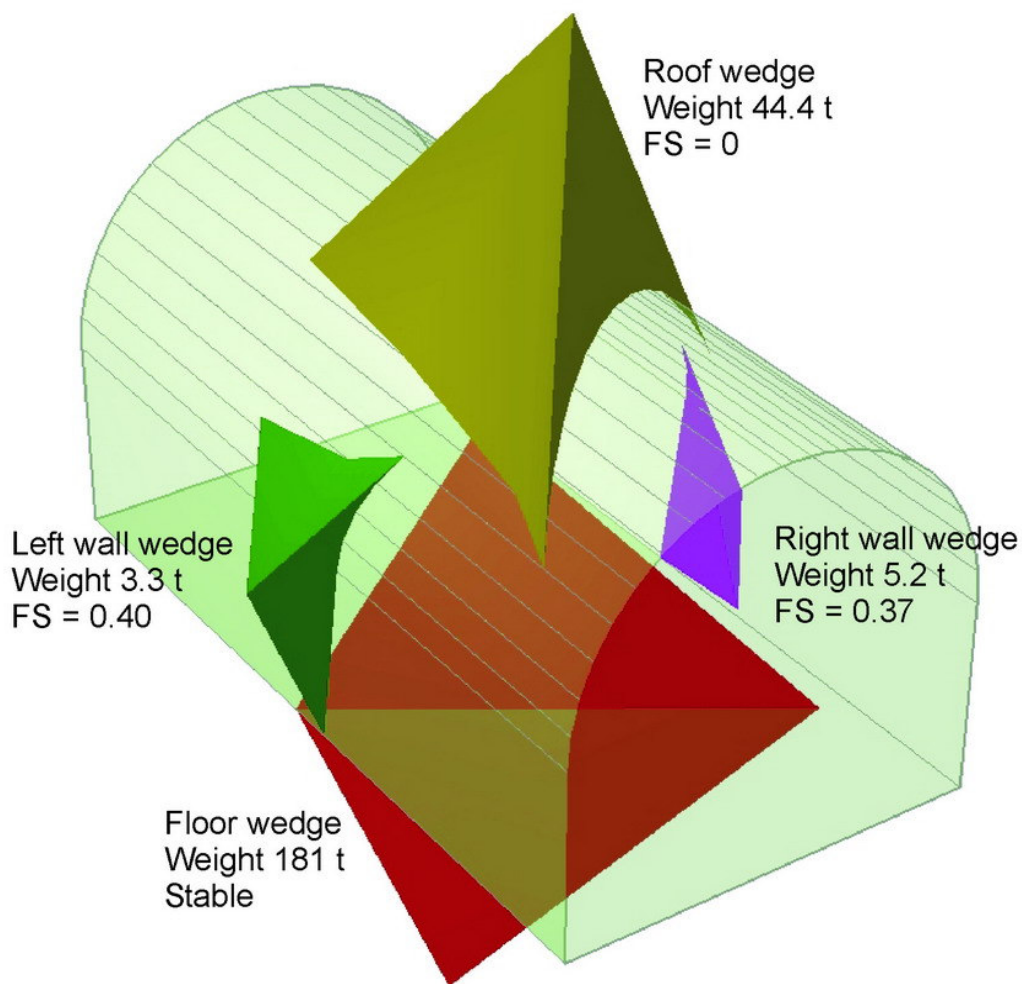


Figure 2: Wedges formed in the roof, floor and sidewalls of a ramp excavated in a jointed rock mass, in which the average dip and dip direction of three dominant structural features are defined by the great circles plotted in Figure 1.

### *Structurally controlled stability in tunnels*

The roof wedge will fall as a result of gravity loading and, because of its shape, there is no restraint from the three bounding discontinuities. This means that the factor of safety of the wedge, once it is released by excavation of the ramp opening, is zero. In some cases, sliding on one plane or along the line of intersection of two planes may occur in a roof wedge and this will result in a finite value for the factor of safety.

The two sidewall wedges are 'cousin' images of one another in that they are approximately the same shape but disposed differently in space. The factors of safety are different since, as shown in the table, sliding occurs on different surfaces in the two cases.

The floor wedge is completely stable and requires no further consideration.

#### **Influence of in situ stress**

The program UNWEDGE can take into account in situ stresses in the rock mass surrounding the opening. For the example under consideration, the influence of in situ stresses can be illustrated by the following example:

Stress	Magnitude	Plunge	Trend
Vertical stress $\sigma_1$	30 t/m <sup>2</sup>	90°	030°
Intermediate stress $\sigma_2$	21 t/m <sup>2</sup>	0°	030°
Minor stress $\sigma_3$	15 t/m <sup>2</sup>	0°	120°

Wedge	Factor of Safety with no in situ stress	Factor of Safety with applied in situ stress
Roof wedge	0	1.23
Right side wedge	0.36	0.70
Side wedge 2	0.40	0.68
Floor wedge	$\infty$	$\infty$

The difference in the calculated factors of safety with and without in situ stresses show that the clamping forces acting on the wedges can have a significant influence on their stability. In particular the roof wedge is stable with the in situ stresses applied but completely unstable when released. This large difference suggests a tendency for sudden failure when the in situ stresses are diminished for any reason and is a warning sign that care has to be taken in terms of the excavation and support installation sequence.

Since it is very difficult to predict the in situ stresses precisely and to determine how these stresses can change with excavation of the tunnel or of adjacent tunnels or openings, many tunnel designers consider that it is prudent to design the tunnel support



on the basis that there are no in situ stresses. This ensures that, for almost all cases, the support design will be conservative.

In rare cases the in situ stresses can actually result in a reduction of the factor of safety of sidewall wedges which may be forced out of their sockets. These cases are rare enough that they can generally be ignored for support design purposes.

### **Support to control wedge failure**

A characteristic feature of wedge failures in blocky rock is that very little movement occurs in the rock mass before failure of the wedge. In the case of a roof wedge that falls, failure can occur as soon as the base of the wedge is fully exposed by excavation of the opening. For sidewall wedges, sliding of a few millimetres along one plane or the line of intersection of two planes is generally sufficient to overcome the peak strength of these surfaces. This dictates that movement along the surfaces must be minimised. Consequently, the support system has to provide a 'stiff' response to movement. This means that mechanically anchored rockbolts need to be tensioned while fully grouted rockbolts or other continuously coupled devices can be left untensioned provided that they are installed before any movement has taken place i.e. before the wedge perimeter has been fully exposed.

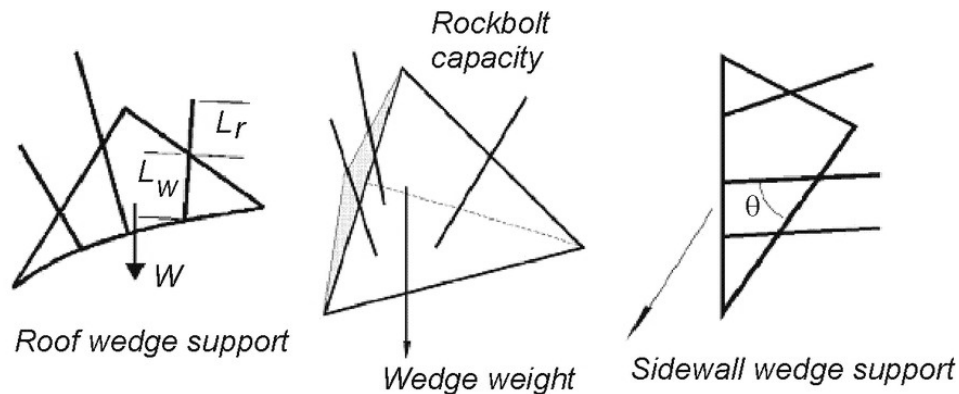


Figure 3: Rockbolt support mechanisms for wedges in the roof and sidewalls of tunnels

### **Rock bolting wedges**

For roof wedges the total force, which should be applied by the reinforcement, should be sufficient to support the full dead weight of the wedge, plus an allowance for errors and poor quality installation. Hence, for the roof wedge illustrated in Figure 3; the total tension applied to the rock bolts or cables should be  $1.3$  to  $1.5 \times W$ , giving factors of safety of  $1.3$  to  $1.5$ . The lower factor of safety would be acceptable in a temporary mine access opening, such as a drilling drive, while the higher factor of safety would be used in a more permanent access opening such as a highway tunnel.

### *Structurally controlled stability in tunnels*

When the wedge is clearly identifiable, some attempt should be made to distribute the support elements uniformly about the wedge centroid. This will prevent any rotations which can reduce the factor of safety.

In selecting the rock bolts or cable bolts to be used, attention must be paid to the length and location of these bolts. For grouted cable bolts, the length  $L_w$  through the wedge and the length  $L_r$  in the rock behind the wedge should both be sufficient to ensure that adequate anchorage is available, as shown in Figure 3. In the case of correctly grouted bolts or cables, these lengths should generally be a minimum of about one metre. Where there is uncertainty about the quality of the grout, longer anchorage lengths should be used. When mechanically anchored bolts with face plates are used, the lengths should be sufficient to ensure that enough rock is available to distribute the loads from these attachments. These conditions are automatically checked in the program UNWEDGE.

In the case of sidewall wedges, the bolts or cables can be placed in such a way that the shear strength of the sliding surfaces is increased. As illustrated in Figure 3; this means that more bolts or cables are placed to cross the sliding planes than across the separation planes. Where possible, these bolts or cables should be inclined so that the angle  $\theta$  is between  $15^\circ$  and  $30^\circ$  since this inclination will induce the highest shear resistance along the sliding surfaces.

The program UNWEDGE includes a number of options for designing support for underground excavations. These include: pattern bolting, from a selected drilling position or placed normal to the excavation surface; and spot bolting, in which the location and length of the bolts are decided by the user for each installation. Mechanically anchored bolts with face plates or fully grouted bolts or cables can be selected to provide support. In addition, a layer of shotcrete can be applied to the excavation surface.

In most practical cases it is not practical to identify individual wedges in a tunnel perimeter and the general approach is to design a rockbolt pattern that will take care of all potential wedges. In the example under consideration the maximum wedge sizes have been identified, as shown in Figure 2, and it has been decided that in situ stresses will not be included in the stability analysis. Consequently, the wedges and their associated factors of safety shown in Figure 2 can be regarded as the most conservative estimate.

Figure 4 shows a typical pattern of 3 m long mechanically anchored 10 tonne capacity rockbolts on a 1.5 x 1.5 m grid. This pattern produces factors of safety of 1.40 for the roof wedge, 3.77 for the right sidewall wedge and 4.77 for the left sidewall wedge.

#### **Shotcrete support for wedges**

Shotcrete can be used for additional support of wedges in blocky ground, and can be very effective if applied correctly. This is because the base of a typical wedge has a large

### *Structurally controlled stability in tunnels*

perimeter and hence, even for a relatively thin layer of shotcrete, a significant cross-sectional area of the material has to be punched through before the wedge can fail.

In the example under consideration, the application of a 10 cm thick shotcrete with a shear strength of  $200 \text{ t/m}^2$  to the roof of the tunnel will increase the factor of safety from 1.40 (for the rockbolted case) to 8.5. Note that this only applies to fully cured (28 day) shotcrete and that the factor of safety increase given by the application of shotcrete cannot be relied on for short term stability. It is recommended that only the rockbolts be considered for immediate support after excavation and that the shotcrete only be taken into account for the long-term factor of safety.

It is important to ensure that the shotcrete is well bonded to the rock surface in order to prevent a reduction in support capacity by peeling-off of the shotcrete layer. Good adhesion to the rock is achieved by washing the rock surface, using water only as feed to the shotcrete machine, before the shotcrete is applied.

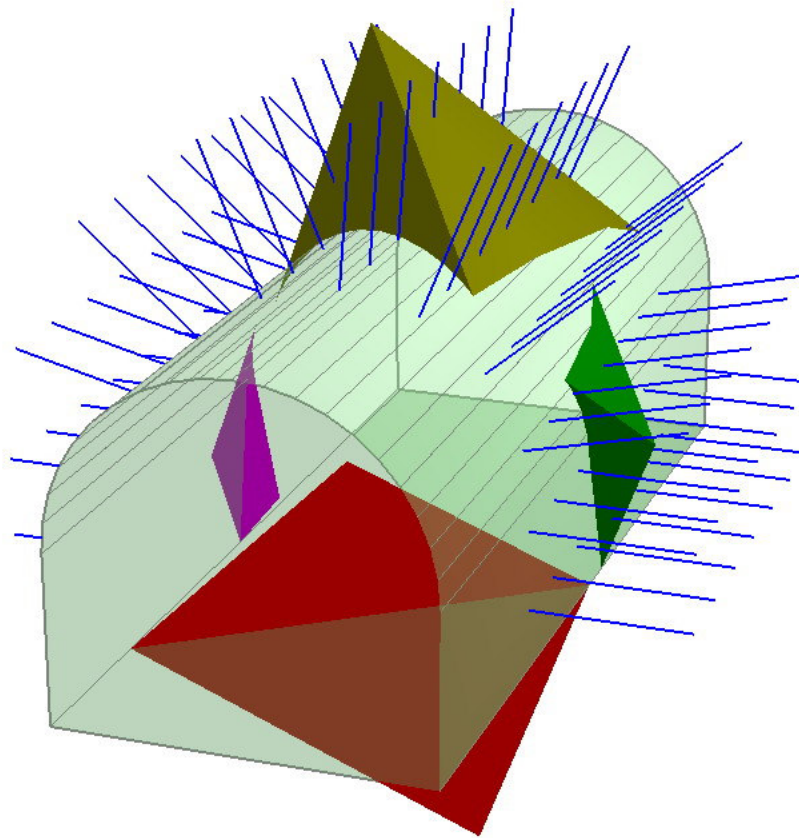


Figure 4: Rock bolting pattern to stabilize the roof and sidewall wedges in the tunnel example discussed earlier.



Figure 5: Ravelling of small wedges in a closely jointed rock mass. Shotcrete can provide effective support in such rock masses

The ideal application for shotcrete is in closely jointed rock masses such as that illustrated in Figure 5. In such cases wedge failure would occur as a progressive process, starting with smaller wedges exposed at the excavation surface and gradually working its way back into the rock mass. In these circumstances, shotcrete provides very effective support and deserves to be much more widely used than is currently the case.

### **Consideration of excavation sequence**

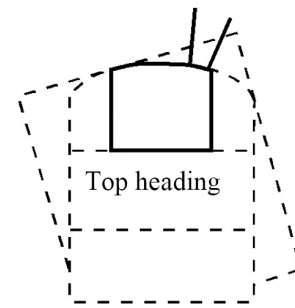
As has been emphasised several times in this chapter, wedges tend to fall or slide as soon as they are fully exposed in an excavated face. Consequently, they require immediate support in order to ensure stability. Placing this support is an important practical question to be addressed when working in blocky ground, which is prone to wedge failure.

When the structural geology of the rock mass is reasonably well understood the program UNWEDGE can be used to investigate potential wedge sizes and locations. A support pattern, which will secure these wedges, can then be designed and rockbolts can be installed as excavation progresses.

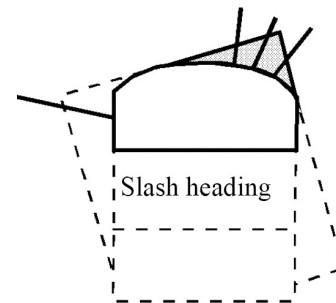
When dealing with larger excavations such as caverns, underground crusher chambers or shaft stations, the problem of sequential support installation is a little simpler, since these excavations are usually excavated in stages. Typically, in an underground crusher chamber, the excavation is started with a top heading which is then slashed out before the remainder of the cavern is excavated by benching.

## Structurally controlled stability in tunnels

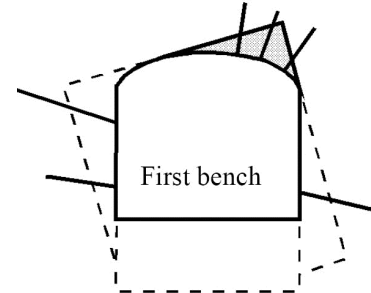
The margin sketch shows a large opening excavated in four stages with rock bolts or cables installed at each stage to support wedges, which are progressively exposed in the roof and sidewalls of the excavation. The length, orientation and spacing of the bolts or cables are chosen to ensure that each wedge is adequately supported before it is fully exposed in the excavation surface.



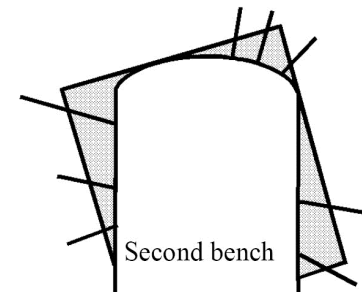
When dealing with large excavations of this type, the structural geology of the surrounding rock mass will have been defined from core drilling or access adits and a reasonable projection of potential wedges will be available. These projections can be confirmed by additional mapping as each stage of the excavation is completed. The program UNWEDGE provides an effective tool for exploring the size and shape of potential wedges and the support required to stabilise them.



The margin sketch shows a support design which is based upon the largest possible wedges which can occur in the roof and walls of the excavation. These wedges can sometimes form in rock masses with very persistent discontinuity surfaces such as bedding planes in layered sedimentary rocks. In many metamorphic or igneous rocks, the discontinuity surfaces are not continuous and the size of the wedges that can form is limited by the persistence of these surfaces



The program UNWEDGE provides several options for sizing wedges. One of the most commonly measured lengths in structural mapping is the length of a joint trace on an excavation surface and one of the sizing options is based upon this trace length. The surface area of the base of the wedge, the volume of the wedge and the apex height of the wedge are all calculated by the program and all of these values can be edited by the user to set a scale for the wedge. This scaling option is very important when using the program interactively for designing support for large openings, where the maximum wedge sizes become obvious as the excavation progresses.



### **Application of probability theory**

The program UNWEDGE has been designed for the analysis of a single wedge defined by three intersecting discontinuities. The “Combination Analyzer” in the program UNWEDGE can be used to sort through all possible joint combinations in a large discontinuity population in order to select the three joints which define most critical wedges.

Early attempts have been made by a number of authors, including Tyler et al (1991) and Hatzor and Goodman (1992), to apply probability theory to these problems and some promising results have been obtained. The analyses developed thus far are not easy to use and cannot be considered as design tools. However, these studies have shown the way for future development of such tools and it is anticipated that powerful and user-friendly methods of probabilistic analysis will be available within a few years.

### **References**

- Hatzor, Y. and Goodman, R.E. 1992. Application of block theory and the critical key block concept in tunneling; two case histories. *In Proc. Int. Soc. Rock Mech. conf. on fractured and jointed rock masses*, Lake Tahoe, California, 632-639.
- Tyler, D.B., Trueman, R.T. and Pine, R.J. 1991. Rockbolt support design using a probabilistic method of key block analysis. In *Rock mechanics as a multidisciplinary science*, (ed. J.C. Roegiers), 1037-1047. Rotterdam: Balkema.
- Tyler, D.B., Trueman, R. and Pine, R.J. 1991. Rockbolt support design using a probabilistic method of key block analysis. *Proc. 32nd U.S. Symp. Rock Mechanics*, Norman, Oklahoma, 1037-47.

# The Rio Grande project - Argentina

## Introduction

The Rio Grande pumped storage project is located on the Rio Grande river near the town of Santa Rosa de Calamucita in the Province of Cordoba in Argentina. It has an installed capacity of 1000 MW and provides electrical storage facilities for the power grid and, in particular, for a nuclear power plant about 50 km away from Rio Grande.

The project is owned by Agua y Energia Electrica, one of the principal Argentinean electrical utility organisations. Preliminary feasibility studies were carried out by the owner and these were followed by detailed design studies by Studio G. Pietrangeli of Rome. The scheme was partly financed by Italy and some of the construction was done by Condote de Agua, an Italian contractor. Golder Associates were involved in the design and supervision of support installed to control the stability of most of the major underground excavations.

The main underground facilities are located in massive gneiss of very good quality. The upper reservoir is impounded behind a rockfill dam and water is fed directly from the intakes down twin penstocks which then bifurcate to feed into the four pump-turbines. These turbines, together with valves and the control equipment, are housed in a large underground cavern with a span of 25 m and a height of 44 m.

Draft tubes from the turbines feed into twin tunnels which, with a down-stream surge shaft, form the surge control system for this project. The twin tunnels join just downstream of the surge tank and discharge into a single tailrace tunnel with a span of 12 m and height of 18 m. This tailrace tunnel is about 6 km long and was constructed by a full-face drill-and-blast top heading, with a span of 12 m and height of 8 m, followed by a 10 m benching operation. A view of the top heading is given in Figure 1.

## Tailrace tunnel support

Because of the excellent quality of the gneiss, most of the underground excavations did not require support and minimal provision for support was made in the contract documents. Assessment of underground stability and installation of support, where required, was done on a 'design-as-you-go' basis which proved to be very effective and economical. Recent reports from site, many years after the start of construction and commissioning of the plant, show that there have been no problems with rockfalls or underground instability.



Figure 1: The 12 m span 8 m high top heading for the tailrace tunnel was constructed by full-face drill-and-blast and, because of the excellent quality of the massive gneiss, was largely unsupported.

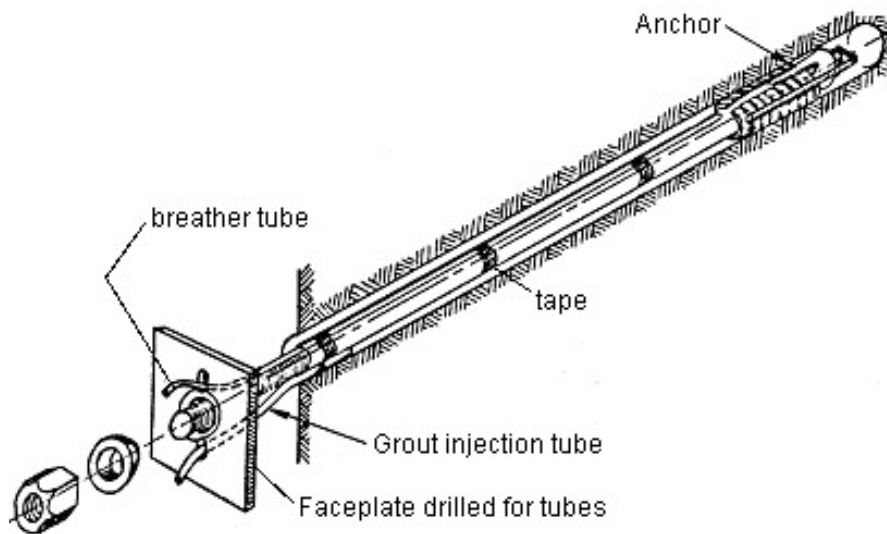


Figure 2: Mechanically anchored rockbolts of the type used on the Rio Grande project. These bolts were tensioned to 70% of their yield load upon installation and then, at a later stage, were re-tensioned and fully grouted.



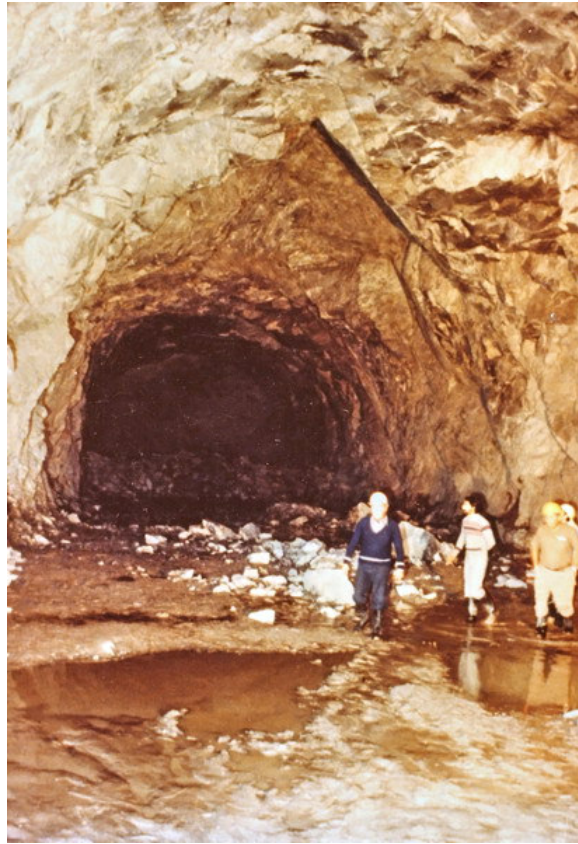


Figure 3: A wedge failure in the roof of the top heading of the Rio Grande tailrace tunnel.

Decisions on support were made on the basis of inspection of the excavated faces by a resident team of geotechnical engineers. Where the appearance of the face indicated that a zone of heavily jointed rock, usually associated with faulting, was being entered, the top heading was reduced to a 6 m span by 8 m high pilot tunnel to limit the volume of unstable rock which could be released from the roof. This pilot tunnel was large enough to accommodate the seven-boom jumbo, as illustrated in Figure 4, but small enough to limit the size of roof falls to manageable proportions. Bolting from inside the pilot heading was used to pre-support the potentially unstable wedges and blocks in the roof.

In the case of the tailrace tunnel, which is itself a large excavation, the support comprised mechanically anchored and cement grouted rockbolts as illustrated in Figure 2, with mesh reinforced shotcrete where required. These bolts were generally installed to control the type of wedge failure illustrated in Figure 3. In the case of particularly large wedges, calculations of the factor of safety and support requirements were carried out on a programmable calculator, using an early version of the program UNWEDGE.



Figure 4: A 6 m wide heading driven ahead of the tunnel face to permit pre-reinforcement of potentially unstable wedges in the roof. The seven-boom jumbo is seen working in the heading.

### **Support for power cavern**

A cross-section of the power cavern is given in Figure 5 and this figure includes the five main excavation stages for the cavern. Careful mapping of significant structural features in the roof and walls of the central access drive at the top of the cavern provided information for estimating potentially unstable blocks and wedges which could form in the roof of the cavern. Figure 6 illustrates a number of such wedges in one section of the cavern roof. At each stage of the cavern excavation, long rockbolts (up to 10 m length) were installed to stabilise wedges or blocks which had been determined as being potentially unstable.

Because gneiss has usually undergone some tectonic deformation during its geological history, projection of structural features from visible exposures tends to be an imprecise process. Consequently, the potentially unstable blocks and wedges had to be reassessed after each excavation step revealed new information. The structural plan illustrated in Figure 6 had to be modified many times during excavation and that shown is the final plan prepared after the full cavern roof had been exposed.

*Rio Grande project - Argentina*

A general view of the cavern excavation is given in Figure 7. This photograph was taken when the bulk of the cavern had been completed and only a few benches in the bottom of the cavern remained to be excavated. The enlarged top of the cavern is to accommodate the overhanging crane that is supported on columns from the cavern floor. An alternative design for this cavern would have been to support the crane on concrete beams anchored to the walls as is commonly done in good quality rock.

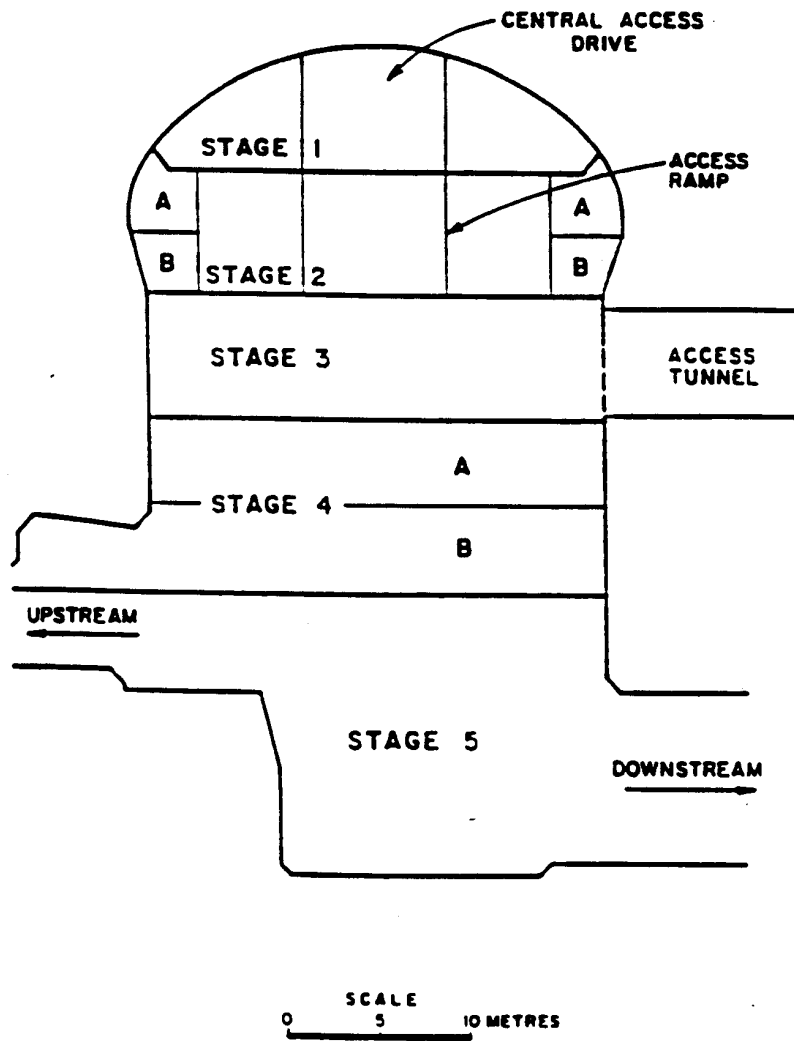


Figure 5: Cavern profile and excavation stages.





Figure 7: A view of the 25 m span Rio Grande power cavern during excavation of the lower benches.

### **Discussion of support design and costs**

Apart from rockbolts installed to control isolated structurally controlled blocks and wedges in the roof and sidewalls and some areas of closely jointed rock which were shotcreted, the cavern was unsupported. While this was successful for this particular project, it is not the approach which should generally be used for a critical excavation such as an underground powerhouse.

## *Rio Grande project - Argentina*

The damage resulting from even a small rockfall in such a cavern is out of all proportion to the savings achieved by eliminating pattern rockbolting and full shotcrete lining. Hence, in addition to the rockbolts installed to control structural instability, as described earlier, I would recommend a normal pattern of 25 mm diameter, 5 m long bolts (20% of the excavation span) on a 2.5 m grid. In addition, I would recommend the placement of 50 mm of fibre-reinforced micro-silica shotcrete over the entire roof and upper sidewalls of the cavern. Based on current north American costs, this additional support, involving approximately 600 rockbolts and about 300 m<sup>3</sup> of shotcrete, would have cost approximately US \$200,000. In terms of the overall project cost and the increased long-term security in the cavern, this would normally be regarded as a good investment.

In contrast, consider the 6 km long tailrace tunnel in which the consequences of a small rockfall are minimal. Assume that a pattern of 4 m long bolts on a 2 m grid (say 10 bolts per section) and a 50 mm shotcrete thickness had been specified for the roof and upper sidewalls of the tailrace tunnel. This would involve 30,000 bolts and 5,400 m<sup>3</sup> of shotcrete at a total cost approaching US \$5 million. This example illustrates the need to give careful consideration to the function and risks associated with each underground excavation before deciding upon the support system to be used.

### **Analysis using UNWEDGE program**

UNWEDGE<sup>1</sup> is a user-friendly micro-computer program which can be used to analyse the geometry and the stability of wedges defined by intersecting structural discontinuities in the rock mass surrounding an underground excavation. The analysis is based upon the assumption that the wedges, defined by three intersecting discontinuities, are subjected to gravitational loading only. In other words, the stress field in the rock mass surrounding the excavation is not taken into account. While this assumption leads to some inaccuracy in the analysis, it generally leads to a lower factor of safety than that which would occur if the in situ stresses were taken into account.

The application of the program UNWEDGE to the analysis of a potentially unstable wedge in the Rio Grande cavern is illustrated in the following discussion.

#### *Input Data*

The dips and dip directions of a number of planes can be entered directly into the table which appears when the 'Input data' option is chosen or this information can be entered in the form of a DIPS file. Once the data has been read into the program, the great circles representing the discontinuities are displayed on the screen as illustrated in Figure 8 and the user is prompted to select the three joint planes to be included in the analysis. Alternatively, the program can be instructed to compute the three most critical planes – those giving the largest wedges with the lowest factors of safety. Once the information on these planes has been entered, the unit weight of the rock

---

<sup>1</sup> Available from [www.rocsience.com](http://www.rocsience.com)

## Rio Grande project - Argentina

and the shear strengths of the joints are entered. Finally, the water pressure acting on the joint surface is entered. In most cases, the default water pressure of 0 will be chosen but the user may check the sensitivity of the wedge to pore water pressure by entering appropriate values.

In the case of the rock mass surrounding the Rio Grande Cavern, the dips and dip directions of the following three sets of joints are included in Figure 8:

- 1 88/225 shear joint set
  - 2 85/264 shear joint set
  - 3 50/345 tension joint set
- Cavern axis: trend 158, plunge 0

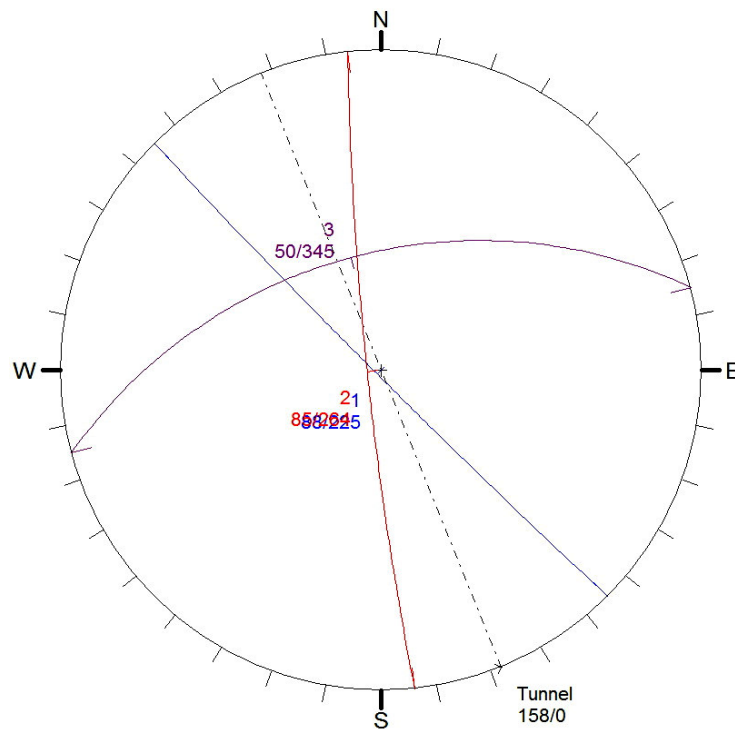


Figure 8: Great circles representing four joint sets which occur in the rock mass surrounding the Rio Grande cavern - imported as a DIPS file.

### *Input of excavation cross-section*

In setting up this analysis, the co-ordinates shown in Figure 9 were used to define the cavern profile. These co-ordinates must be entered sequentially and must form a closed figure. The profile is formed from straight line and arc segments and a sufficient number of co-ordinates should be entered to ensure that a smooth profile is generated.

*Determination of wedge geometry*

Depending upon the shape of the cross-section, a maximum of six wedges can be formed with three intersecting joint planes. Selecting the '3D wedge view' option gives a number of views showing the shape and size of these wedges. The two wedges formed on the cavern end walls can be viewed by activating the 'End wedges' option.

Figure 10 shows the wedges formed in the case of the Rio Grande power cavern for the three joint planes defined in Figure 8. The weight of each of these wedges, the failure mode and the calculated factor of safety are shown in the figure. Obviously, the most dangerous wedge in this situation is the wedge formed in the roof while the wedge formed in the floor is stable and need not be considered further in this analysis.

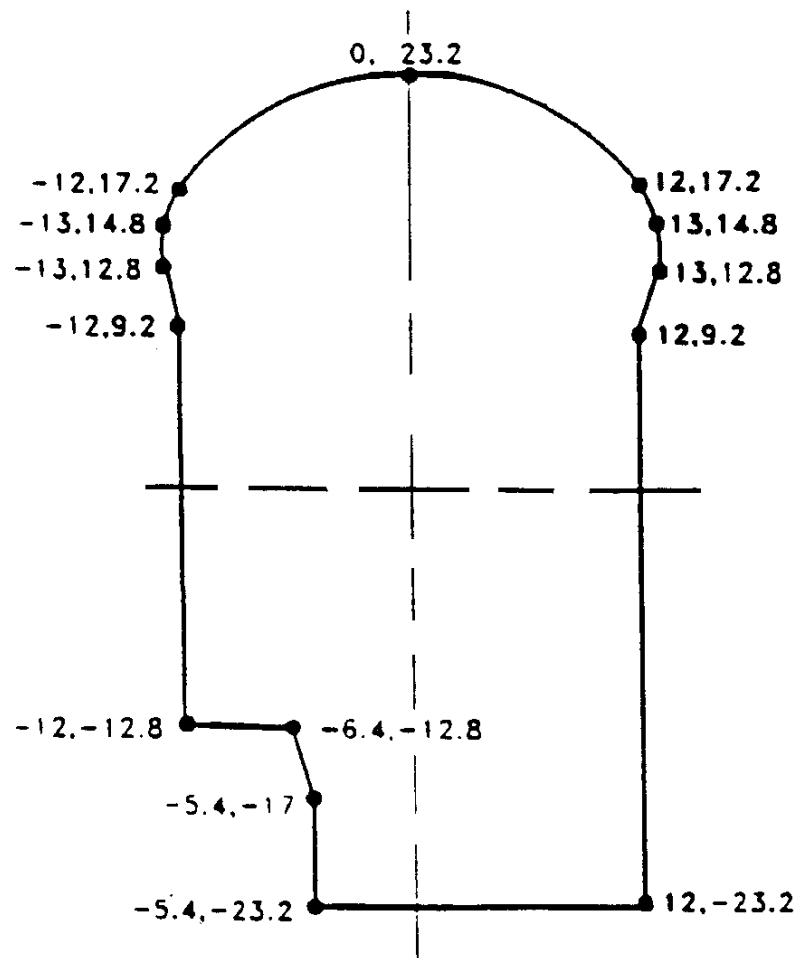


Figure 9: Co-ordinates used to define the profile of the cavern.



## Rio Grande project - Argentina

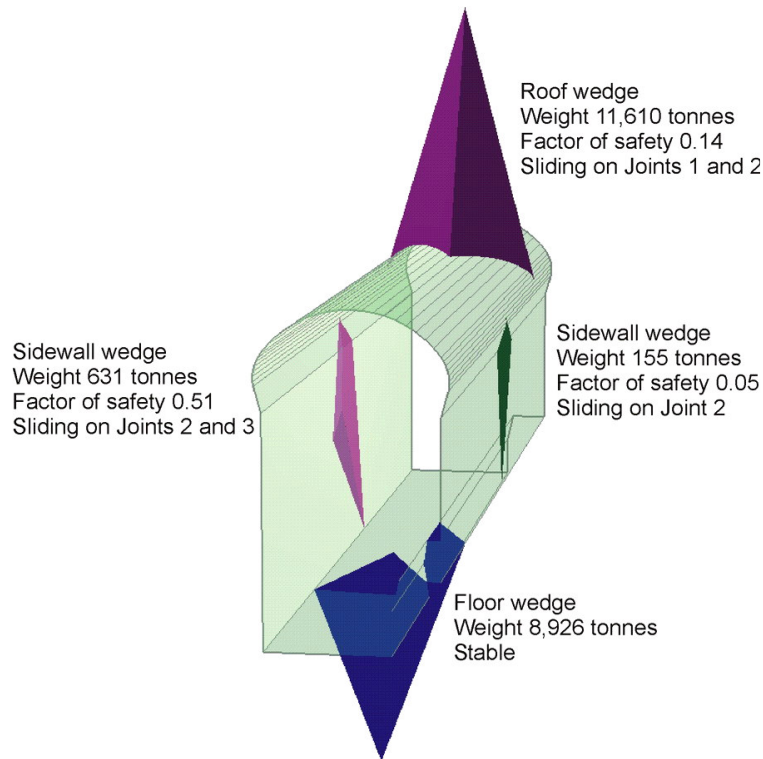


Figure 10: Perspective view of the wedges formed in the rock mass surrounding the Rio Grande power cavern.

### *Sizing of wedges*

The program UNWEDGE automatically determined the largest wedge that can occur in the rock mass adjacent to the excavation profile. In the case of the roof wedge, shown in Figure 10, the wedge extends over the full 25 m span of the cavern and weighs 11,610 tonnes. While, in exceptional circumstances, such wedges may occur, the limited extent of joints in many rock masses will restrict the size of the wedges to much smaller dimensions than those determined by UNWEDGE for the large excavations.

As illustrated in Figure 6, the trace length of joint number 3 (50/345) in the upper roof wedge is approximately 6 m. When the 'Scale wedges' is chosen, the user can define the size of the wedge in terms of the area of the face on the excavation surface, the volume of the wedge, the height of the apex of the wedge, the length of one of the joint traces or the persistence of one of the joints. In this case a trace length of 6 m is entered for joint number 3, defined by 50/345, and the resulting wedge is illustrated in Figure 11. This wedge weighs 220 tonnes and will require about seven 50 tonne capacity fully grouted cables to give a factor of safety of about 1.5 which is considered appropriate for a cavern of this type.

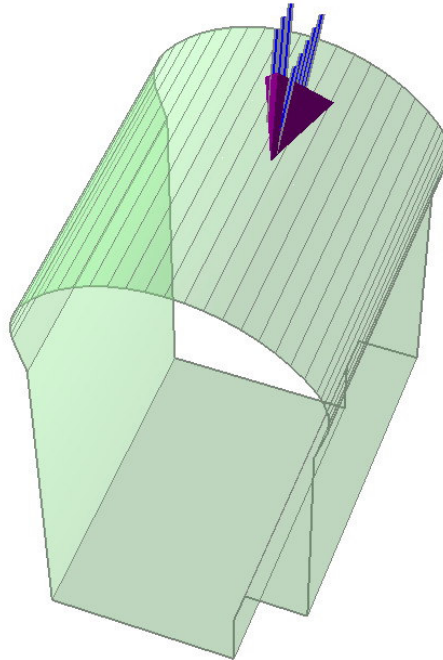


Figure 11: Perspective view of roof wedge in the Rio Grande cavern roof. The size of this wedge has been defined by setting the trace length of the 50/345 joint to 6 m. Eight 10 m long 50 tonne capacity grouted anchors give a factor of safety of 1.6 .

UNWEDGE allows the user to add a layer of shotcrete and calculates the factor of safety increase as a result of such an addition. Since the shotcrete can only be added once the surface of the wedge is fully exposed it is not taken into account in calculating the support required to stabilise the wedge. The increase in safety factor which occurs after the shotcrete has set can be regarded as a long term bonus and it does allow the user to choose a slightly lower factor of safety for the immediate support of the wedge.



## Dr. Evert Hoek: Experience and Expertise

Evert Hoek was born in Zimbabwe, graduated in mechanical engineering from the University of Cape Town and became involved in the young science of rock mechanics in 1958, when he started working in research on problems of brittle fracture associated with rockbursts in very deep mines in South Africa.

His degrees include a PhD from the University of Cape Town, a DSc (eng) from the University of London, and honorary doctorates from the Universities of Waterloo and Toronto in Canada. He has been elected as a Fellow of the Royal Academy of Engineering (UK), a Foreign Associate of the US National Academy of Engineering and a Fellow of the Canadian Academy of Engineering.

Dr. Hoek has published more than 100 papers and 3 books. He spent 9 years as a Reader and then Professor at the Imperial College of Science and Technology in London, 6 years as a Professor at the University of Toronto, 12 years as a Principal of Golder Associates in Vancouver, and the last 17 years as an independent consulting engineer based in North Vancouver. His consulting work has included major civil and mining projects in 35 countries around the world and has involved rock slopes, dam foundations, hydroelectric projects, underground caverns and tunnels excavated conventionally and by TBM.

Dr. Hoek has now retired from active consulting work but, in 2010, is still a member of consulting boards on three major civil and mining engineering projects in Canada, the USA and Chile.

